Generalized potential description of the interaction of very light clusters: scattering and photonuclear reactions

V. G. Neudachin, A. A. Sakharuk, and Yu. F. Smirnov
Institute of Nuclear Physics, Moscow State University, Moscow

Fiz. Elem. Chastits At. Yadra **23**, 479–541 (March–April 1992)

In the $SU(4)$ supermultiplet symmetry approximation the problem of the interaction of clusters A and B can be reduced to a set of one-channel scattering problems with potentials $V^{[f]}$, where $[f]$ are the allowed Young schemes for the system $A+B$. This is important for channels with minimum total spin S, where the nonunitary elastic scattering amplitude T_{LS} is the half-sum of two strongly differing amplitudes $T_L^{[f]}$, and the inelastic amplitude with spin–isospin flip of the deuteron or deuteron charge exchange is the half-difference. The cluster pairs $d+t$, $d+p$, $p+t(h)$, and $d+d$ are studied. A good description of the available experimental data on the elastic and inelastic cross sections is obtained and many predictions are made. These pairs of clusters are interesting for the physics of thermonuclear reactions. The potentials that are obtained are defined both as the momentum distribution of the clusters in the initial state and as their final-state interaction in the case of photonuclear reactions. The technique of preparation of continuum states with a specified symmetry $[f]$ is outlined. Comparison with experiment shows that quantitative agreement is obtained.

INTRODUCTION

The nearly twenty-year-old potential description of the scattering of light clusters[1–4] such as $\alpha+\alpha$, $h+t(h)$, $\alpha+t(h)$, and $\alpha+d$ was based on the idea of deep attractive potentials with forbidden states. This description was the generalization of an important preceding step—the orthogonality-condition model.[5] Besides revealing the very simple physics of the scattering process compared with the widely used resonating-group method (RGM),[6] the potential description produced an important new result: for the first time it was shown that the E dependence of the phase shifts $\delta_L(E)$ obeys the generalized Levinson theorem.[7] All the important phases are positive, and as the energy increases from zero they begin from different values $(n+m)\pi$ (n is the number of observed bound states, and m is the number of bound states of the potential but forbidden by the Pauli principle). In the end, as E increases they enter the general region of Born values $\delta_L(E)<1$. This implied a fundamental revision of the overall picture compared with the RGM picture, where it was assumed either directly or indirectly that the cluster interaction has a repulsive core, since the scattering phases for $E_{\text{c.m.}}>5$–10 MeV were assumed to be negative. For all the pairs of nuclei listed above, effects of nonlocality of the potential, expressed, for example, in the damping of the wave function at small distances, are small. They begin to play an important role in $^{16}O+^{16}O$ scattering.[8]

This potential description was later widely used for various purposes: in the experimental study of $\alpha+\alpha$ scattering at energies E_{lab} up to 400 MeV (Ref. 9); as a model for solving the inverse scattering problem;[10] as the first example of a deep attractive potential in composite-particle interactions in reinterpreting the data on heavy-ion interactions, where during the last ten years the repulsive core has been rejected in favor of deep attractive potentials,[8,11,12] as discussed by us in Ref. 13; in the study of the 3α system[14] and the ^{9}Be nucleus as the system $\alpha+\alpha+n$ (Ref. 15); as the basis for the theoretical explanation of photodisintegration $^7\text{Li}\gamma\to\alpha+t$ or $^6\text{Li}\gamma\to\alpha+d$, where the cross section falls off relatively slowly with increasing energy, since in the ground state of ^{7}Li there is a node in the P wave in the $\alpha+t$ relative motion, i.e., there is enrichment by large momenta;[16] as the first example in the reinterpretation of the NN interaction as the interaction of composite quark-containing particles.[17]

Meanwhile, for unclear reasons this very effective potential description was not widely used in the scattering of the lightest clusters such as $d+d$, $p(n)+d$, $p(n)+t(h)$, and $d+t(h)$. This "conspiracy of silence" was justified, since the description of such systems required an important step which was unknown earlier: the introduction, into certain channels with given total orbital angular momentum L and total spin S of interference between the two potential amplitudes corresponding to two different Young schemes $[f]$. This was done in our studies of Refs. 18–20.

The introduction of a dependence of the potential on the symmetry $[f]$ is justified when this dependence is strong and determines important qualitative features of the interaction. This was precisely the situation in the systems that we considered. Typically, in the few studies[21,22] in which the $p+d$ system was not studied using the supermultiplet description with interference of potential amplitudes with different symmetries $[f]$ in channels with $S=\frac{1}{2}$, unsuccessful attempts were made to combine the potential description of the ground state of the ^{3}He nucleus as a $p+d$ system and $p+d$ scattering in a fairly wide energy range. The problem is that if the ground state of the ^{3}He nucleus accurately corresponds to the symmetry $[f]=[3][23]$, then in the continuum for channels with $S=\frac{1}{2}$ we have a superposition of the symmetries $[f]=[3]$ and $[f]=[21]$ with equal weights!

 0090-4759/92/020210-29$04.00

Our approach concerns direct nuclear processes, and, as we shall see, is well justified. But formally it is directly related to the studies of Ref. 24, where the decay of quasistationary states of light nuclei was studied assuming that these states are characterized by the Young scheme $[f]$, which is a good quantum number. However, when the level density is high (even in a nucleus such as ^{4}He at excitation energies $E^* \cong 25$ MeV), this assumption is not valid (as in the case of the levels of the ^{8}Be nucleus at energies $E^* \cong 16$–17 MeV, the isospin T is not conserved[25]).

Regarding the more detailed comparison of the systems that we consider here with systems such as $\alpha+\alpha$, we note that the $\alpha+\alpha$ system is characterized by only a single Young scheme $[f]=[44]$, and all the angular momenta L are even. For the system $\alpha+t$ again only one symmetry $[f]=[43]$ is allowed, but there are both even and odd orbital angular momenta L, and splitting of the potential in the parity of L occurs (as for the system $\alpha+d$). This effect leads to an increase in the scattering cross section in the backward hemisphere.[11] The next stage of complication is the system $t+h$, where the Young scheme $[f]=[42]$ corresponds to even L and $[f]=[3]$ corresponds to odd L (see Refs. 4, 26, and 27 on these questions), but here a single Young scheme $[f]$ corresponds to a channel with given values of L and S. But in the system $d+d$, for example, we encounter a much more complicated and interesting situation: two Young schemes $[f]=[22]$ and $[f]=[4]$ are possible in each of the channels with even L and $S=0$, and therefore, as will become clear, the phase shifts are composite. In fact,

$$\boxed{1}\boxed{2} \times \boxed{3}\boxed{4} = \boxed{1}\boxed{2}\boxed{3}\boxed{4} + \begin{array}{|c|c|c|}\hline 1&2&3\\\hline 4\\\cline{1-1}\end{array} + \begin{array}{|c|c|c|}\hline 1&2&4\\\hline 3\\\cline{1-1}\end{array} + \begin{array}{|c|c|}\hline 1&2\\\hline 3&4\\\hline\end{array}\ , \tag{1}$$

where even permutations $(12)\leftrightarrow(34)$ (change of sign of the radius vector), i.e., the Young schemes $[f]=[4]$ and $[f]=[22]$, must correspond to even L, and odd permutations, i.e., $[f]=[31]$ (see Ref. 28 for the Young scheme) must correspond to odd L. Since deuterons are bosons, $S=0$ and 2 can correspond to even L, and $S=1$ to odd L (this is related to the symmetry properties of the Clebsch–Gordan coefficients). The antisymmetry of the full wave function in the four nucleons causes the value $S=2$ to be incompatible with the orbital symmetry $[f]=[4]$, since the spin–isospin symmetries have the form $[f_S]=[4]$, $[f_T]=[4]$.

The lightest p-shell nucleus possesses a very clearly expressed supermultiplet structure,[29] characterized, for example, by the fact that a large energy $\Delta E \cong 15$ MeV is needed to break the Young scheme $[f]=[4]$. The important role played by this fact in the theory of nuclear reactions involving very light nuclei has been analyzed repeatedly in the literature.[30–34] Continuing this line of investigation, we base our work on the concept of a reaction amplitude with fixed total Young scheme $[f]$ and take a natural step forward: we represent the total scattering amplitude as a superposition of amplitudes with different Young schemes $[f]$ (Ref. 18). Here it is important that the scattering amplitude in channels with even L and $S=2$ is unitary, since the Young scheme $[f]$ has the single value $[f]=[22]$. Consequently, in determining the potential $V^{[22]}(r)$ we take the corresponding phases from experiment[35] and the RGM calculations for the dd system[36] (redefining the phases by means of a suitable term $n\pi$ owing to the presence of a forbidden state). A similar situation occurs in odd waves with odd L and $S=1$, where $[f]=[31]$. Meanwhile, for channels with even L and $S=0$ we have a superposition of potential amplitudes $T_L^{[f]}$ with the symmetries $[f]=[4]$ and $[f]=[22]$. This creates a very interesting situation which has not been discussed before. An inelastic channel with spin–isospin flip, $dd\to d_s d_s$, appears, where d_s is the singlet deuteron. The amplitude of this inelastic channel is $\frac{1}{2}(T_L^{[4]}-T_L^{[22]})$. At $E_{\text{c.m.}} \cong 6$ MeV the elastic nonunitary amplitude $T_L=\frac{1}{2}(T_L^{[4]}+T_L^{[22]})$ for $L=0$ and 2 is close to zero, owing to the destructive interference of the two potential amplitudes, which arises because of the very strong difference between the potentials $V^{[4]}(r)$ and $V^{[22]}(r)$. As a result, in this region there is no interesting composition law for the phase shifts of elastic singlet scattering $2\delta_L=\delta_L^{[4]}+\delta_L^{[22]}$ which could allow us to determine the phase shifts $\delta_L^{[4]}$ from the known phase shifts δ_L for $S=0$ and 2. Nevertheless, the potential $V^{[4]}(r)$ is determined fairly reliably by the two levels 0_1^+ and 0_2^+ of the ^{4}He nucleus and by the fact that there is apparently a D state at energies of 3–6 MeV above the $\alpha\to d+d$ threshold. The 0_2^+ level is characterized by a large spectroscopic factor $S_{tp} \cong 1$, which suggests that $S_{dd} \cong 1$, as occurs for the 0_1^+ ground state (in the ^{6}Li nucleus the spectroscopic factors $S_{\alpha d}$ and S_{ht} are also large).

The scheme described here is valid also for other pairs of very light nuclei $p+d$, $t+h$, $t+d$, and related ones.

1. THE FORMAL METHOD

Assuming $SU(4)$ symmetry,[39,31] we have the obvious expansion of the partial $A+B$ scattering amplitude:

$$\begin{aligned} T_L = \sum_{s,\sigma,t,\tau,[f]} & (t_A\tau_A, t_B\tau_B | t\tau)(S_A\sigma_A, S_B\sigma_B | S\sigma) \\ & \times \langle [\tilde{f}_A] S_A t_A, [\tilde{f}_B] S_B t_B | [\tilde{f}] \times St \rangle \\ & \times T_L^{[f]} \langle [\tilde{f}] St | [\tilde{f}_A] S'_A t'_A, [\tilde{f}_B] S'_B t'_B \rangle \\ & \times (S\sigma | S'_A \sigma'_A, S'_B \sigma'_B)(t\tau | t'_A \tau'_A, t'_B \tau'_B). \end{aligned} \tag{2}$$

Here S, t, and $[\tilde{f}]$ are the spin, isospin, and spin–isospin Young scheme of the system $A+B$; σ and τ are the spin and isospin projections, respectively, and $\langle [\tilde{f}_A] S_A t_A, [\tilde{f}_B] S_B t_B | [\tilde{f}] St \rangle$ are the isoscalar factors of the Clebsch–Gordan coefficients of the group $SU(4)$ (Ref. 37). The quantities $T_L^{[f]}$ are the parts of the T matrix invariant under $SU(4)$ transformations.

The partial amplitudes T_L determine the expansion of the total scattering amplitude $f(\vartheta)$ in orbital angular momenta L:

$$f(\vartheta)=-\frac{i}{2p_0}\sum_L (2L+1)T_L P_L(\cos\theta),$$

where p_0 is the momentum of the relative motion of particles A and B in the c.m. frame.

The cross section for elastic scattering (both elastic and with "soft" rearrangement of the spin–isospins of particles A and B without change of their Young schemes), averaged over the initial orientations of the spins σ_A and σ_B and summed over the final ones σ'_A and σ'_B (we consider the scattering of polarized particles), has the form

$$\frac{d\sigma}{d\Omega}(\vartheta)=\frac{1}{(2S_A+1)(2S_B+1)}\sum_{\sigma_A,\sigma_B,\sigma'_A,\sigma'_B}|f(\vartheta)|^2$$

$$=\frac{1}{4p_0^2}\sum_{l=0}^{\infty}B_l P_l(\cos\vartheta),$$

$$B_l=\frac{1}{(2S_A+1)(2S_B+1)}\sum_{L=0}^{\infty}\sum_{L'=|L-l|}^{L+l}(2L+1)$$

$$\times(2L'+1)(L0,L'0|l0)^2\sum_{\substack{[f],t,\tau\\ [f'],t',\tau'}}(t_A\tau_A,t_B\tau_B|t\tau)$$

$$\times(t'_A\tau'_A,t'_B\tau'_B|t'\tau')(t_A\tau_A,t_B\tau_B|t\tau)$$

$$\times(t'_A\tau'_A,t'_B\tau'_B|t'\tau')\sum_S(2S+1)T^{[f]}_{L,t,S}$$

$$\times[T^{[f']}_{L',t',S}]^*\langle[\tilde f_A]S_At_A,[\tilde f_B]S_Bt_B|[\tilde f]\times St\rangle^2$$

$$\times\langle[\tilde f_A]S'_At'_A,[\tilde f_B]S'_Bt'_B|[\tilde f']St'\rangle^2. \qquad (3)$$

We shall familiarize ourselves with this general expression by studying special cases. In particular, for $d+d$ scattering

$$B_l=\frac{1}{(2S_d+1)^2}\sum_{L=0}^{\infty}\sum_{L'=|L-l|}^{L+l}(2L+1)(2L'+1)$$

$$\times(L0,L'0|l0)^2\sum_{[f],[f']}(2S+1)T^{[f]}_L T^{[f']*}_{L'}$$

$$\times\sum_S(2S+1)\langle[\tilde 2]10,[\tilde 2]10|[f]S0\rangle^2$$

$$\times\langle[\tilde 2]10,[\tilde 2]10|[\tilde f']S0\rangle^2, \qquad (4)$$

where we must use the following nonzero isoscalar factors:[37]

$$\langle[\tilde 2]10,[\tilde 2]10|[\tilde{22}]00\rangle=\sqrt{1/2},$$

$$\langle[\tilde 2]10,[\tilde 2]10|[\tilde 4]00\rangle=\sqrt{1/2},$$

$$\langle[\tilde 2]10,[\tilde 2]10|[\tilde{31}]10\rangle=1,$$

$$\langle[\tilde 2]10,[\tilde 2]10|[\tilde{22}]20\rangle=1. \qquad (5)$$

We write the amplitude $T^{[f]}_L$ as the potential amplitude (see the Introduction)

$$T^{[f]}_L=\exp(2i\delta^{[f]}_L)-1, \qquad (6)$$

and immediately find from (4) and (5) that for $S=0$ and, accordingly, for even L

$$T_{L,S=0}=\tfrac12(T^{[4]}_L+T^{[22]}_L). \qquad (7)$$

Going to the S matrix, for elastic scattering we have

$$S^{el}_{L,S}=\eta_{L,S}\exp(2i\delta_{L,S})\equiv T_{L,S}+1,$$

$$\eta_{L,S=0}=|\cos(\delta^{[4]}_L-\delta^{[22]}_L)|, \qquad (8)$$

$$\delta_{L,S=0}=\tfrac12\delta^{[4]}_L+\tfrac12\delta^{[22]}_L. \qquad (9)$$

The nonunitarity of the elastic scattering amplitude implies the opening of the charge-exchange channel $d+d\to nn+pp$ and the channel with flip of the deuteron spin–isospin, $d+d\to d_s+d_s$:

$$S^{flip}_{L,S=0}=(10,10|00)(\tfrac12T^{[4]}_L-\tfrac12T^{[22]}_L),$$

$$S^{c}_{L,S=0}=(11,1-1|00)(\tfrac12T^{[4]}_L-\tfrac12T^{[22]}_L) \qquad (10)$$

(these expressions contain the Clebsch–Gordan spin–isospin coefficients),

$$|S^{el}_{L,0}|^2+|S^{flip}_{L,0}|^2+2|S^{c}_{L,0}|^2=1,$$

$$|S^{el}_{L,1}|^2=1,\quad |S^{el}_{L,2}|^2=1.$$

The expression for "almost elastic" $A+B$ scattering with change of only the spin–isospins of particles A and B (when at least one of them is a deuteron) has the form

$$\frac{d\sigma}{d\Omega}(\vartheta)=\frac{1}{4p_0^2}\frac{(2S'_A+1)(2S'_B+1)}{(2S_A+1)(2S_B+1)}(t'_A\tau'_A,t'_B\tau'_B|t\tau)^2$$

$$\times\Big|\sum_L(2L+1)P_L(\cos\vartheta)$$

$$\times\{\langle[\tilde f_A]S_At_A,[\tilde f_B]S_Bt_B|[\tilde f_1]St\rangle$$

$$\times\langle[\tilde f_A]S'_At'_A,[\tilde f_B]S'_Bt'_B|[\tilde f_1]St\rangle T^{[f_1]}_L$$

$$+\langle[\tilde f_A]S_At_A,[\tilde f_B]S_Bt_B|[\tilde f_2]St\rangle$$

$$\times\langle[\tilde f_A]S'_At'_A,[\tilde f'_B]S'_Bt'_B|[\tilde f_2]St\rangle T^{[f_2]}_L\}\Big|^2. \qquad (11)$$

Here $S_B=1$, $S'_B=0$, $t'_B=1$, $[\tilde f_B]=[\tilde 2]$, $t_B=0$, $[\tilde f_B]=[\tilde 2]$, $S_A=\frac12$, $S'_A=\frac12$, $t_A=\frac12$, $t'_A=\frac12$, $[f_A]=[f_A]=[\tilde 1]$, $t=\frac12$, $\tau=\frac12$, and $S=\frac12$ for the $p+d$ and $d+h$ systems; $S_A=1$, $S'_A=0$, $t_A=0$, $t'_A=1$, $[\tilde f_A]=[\tilde f_A]=[\tilde 2]$, $t=0$, $\tau=0$, and $S=0$ for the $d+d$ system. Here if spin–isospin flip of the deuteron occurs without charge exchange, $\tau'_A=\frac12$, $\tau'_B=0$ for the $p+d$ and $d+h$ systems and $\tau'_A=\tau'_B=0$ for the $d+d$ system. If charge exchange does occur, then $\tau'_A=\frac12$, $\tau'_B=1$ for the $p+d$ and $d+h$ systems and $\tau'_A=1$, $\tau'_B=-1$ for the $d+d$ system.

The expressions given above generalize the well known Lane approach[38] to optical scattering, where the term $(T\tau)$ is related to the charge-exchange cross section and the corresponding contribution to the elastic scattering amplitude. Below, we shall see for our first example, $d+d$, that the phases $\delta^{[4]}_L$ and $\delta^{[22]}_L$ differ strongly, so that Eqs. (8)–(11) are essential for the physics, and it is important to carry out the corresponding measurements of the cross

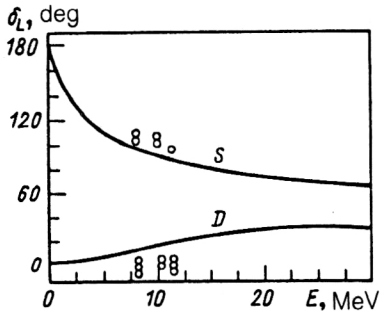

FIG. 1. Phase shift for the potential $V^{[22]}(r)$. Experimental data from Ref. 34.

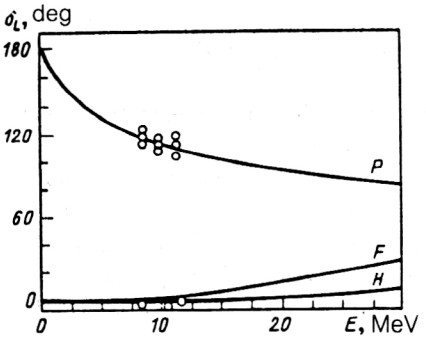

FIG. 3. Phase shifts for the potential $V^{[31]}(r)$. Experimental data from Ref. 34.

section for the reaction $d_s \to d_s$. Below the $d+d \to d_s+d_s$ threshold, instead of Eq. (8) we should have $\eta_{L,S=0}=1$, and the validity of Eq. (9) is a separate question. Equation (10) shows that the cross sections for inelastic processes are expressed in terms of the phase shifts of elastic scattering for the *dd* interaction.

2. RECONSTRUCTION OF THE *dd* INTERACTION POTENTIAL

Now for the example of the *dd* system let us discuss the approach to the experimental data and the problem of reconstructing the potentials $V^{[f]}(r)$, with $[f]=[4]$, $[f]=[31]$, and $[f]=[22]$. We begin with the $S=2$, even-L "potential" channels, where only the single Young scheme $[f]=[22]$ is allowed. Experimental data on the phase shifts[35] are difficult to obtain, since the S matrix for the elastic scattering of two particles with unit spin involves many parameters. There are several mixing angles, and polarization experiments are required even in a simplified treatment where the mixing angles are neglected. These experimental data (which exist in the narrow range $E_{\text{c.m.}}=4$–6 MeV) are in good agreement with the RGM calculation.[36] In choosing the potential we start from the requirement that it have a forbidden S state, since the Young scheme $[f]=[22]$ can be realized beginning with the configuration s^2p^2 (see the analog in Ref. 26). Meanwhile, the known 0_2^+ (20.1 MeV) state does not correspond to the Young scheme $[f]=[22]$, since it decays via the $t+p$ channel with the large spectroscopic factor $S_p \cong 1$ (Ref. 39) and is related in the literature[40] to the symmetry

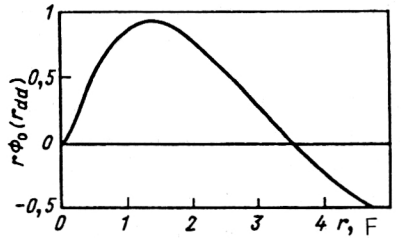

FIG. 2. Wave function of S-wave scattering for the potential $V^{[22]}(r)$ for $E_{\text{c.m.}}=0.5$ MeV.

$[f]=[4]$ (we shall use this fact below). The set of phase shifts (even in a narrow energy range) for three values of the orbital angular momentum $L=0,2,4$, together with the fact that a forbidden S state exists uniquely determines the parameters of the *dd* interaction potential for the symmetry $[f]=[22]$:

$$[f]=[22], \quad V_0=-41.5 \text{ MeV},$$
$$R_0=1.45 \text{ F}, \quad a=0.81 \text{ F} \qquad (12)$$

(here we have in mind a potential of the Woods–Saxon type). The results of calculating the phase shifts with the potential (12) plus the Coulomb interaction are shown in Fig. 1, where we see that the description is qualitatively good (for channels with $S=2$ and even L). In Fig. 2 we show the wave function for the S wave at low energy $E_{\text{c.m.}}=0.5$ MeV. The node of this wave function at the radius $r=3.2$ F (reflecting the existence of a forbidden S state) was perceived earlier[33] (exactly as in $\alpha\alpha$ scattering[26]) as a repulsive core, whose radius $r_0 \cong 4$ F was determined from the slope of the S-wave phase shift at low energies.

Turning now to other channels with the potential description characterized by the quantum numbers $S=1$, odd L, and $[f]=[31]$, we have the simplest realization of this symmetry in the shell configuration s^3p, from which we conclude that there are no forbidden states in the potential $V_L^{[31]}(r)$. In Fig. 3 we show that the potential is well determined by the experimental values of the P- and F-wave phase shifts. In particular, the P-wave phase shift at zero energy begins from the value $\delta_1=\pi$. The unknown potential corresponding to the results in Fig. 3 has the parameters

$$[f]=[31], \quad V_0=-31.8 \text{ MeV},$$
$$R_0=2.33 \text{ F}, \quad \alpha=0.76 \text{ F}. \qquad (13)$$

It gives a good description of the experimental data and predicts a behavior of the phase shifts at higher energies in good agreement with the RGM (as in Fig. 1).[36] We neglect a splitting of the P-wave phase shift in the total angular momentum J, which, as shown by the experiment of Ref. 35, does not exceed 10° at energies $E_{\text{c.m.}}>6$ MeV. Meanwhile, at low energies $E_{\text{c.m.}} \to 0$ the phase shifts ${}^J\delta_L$ for

$L=1$ and $J^\pi=0^-$ and 2^- become ${}^J_S\delta_L=\pi$ (there are weakly coupled states[39]), and a quasistationary state corresponds to $J^\pi=1$ (Ref. 39). This difference is interpreted as the effect of the tensor NN interaction. For a more accurate description it is not difficult to introduce into our scheme the J splitting of the depth of the potential $V^{[31]}(r)$: $V_0=V_{00}+(-1)^J\Delta V_0$.

Let us now turn to the problem of the dd potential $V^{[4]}(r)$. Here it is natural to base our analysis on the following:

1. The ground state of the ^{4}He nucleus is a strongly coupled state in the potential $V^{[4]}(r)$.

2. The above-mentioned excited state 0^+(20.1 MeV) of the ^{4}He nucleus is an excited state in this potential [the wave function $\Phi_{NL}(r_{dd})$ with a node, $N=2$, $L=0$]. It is true that for this state there are no experimental data on the spectroscopic factor $S_{dd}[^4\text{He}^*(0^+)]$ of its virtual decay into two deuterons. This spectroscopic factor must be close to unity in the potential model (as occurs for the ground state of the ^{4}He nucleus). These two facts already specify the parameters of the potential $V^{[4]}(r)$ very closely, even if we do not attempt to reproduce the energy of the 0_2^+(20.1 MeV) level very accurately (i.e., the binding energy of this level is 3.7 MeV in the $d+d$ system). This level apparently has a fairly complicated wave function,[40] even when the spectroscopic factor S_{dd} approaches unity.

3. It would appear that the primary role must be played by the analysis of the phase shifts in the $S=0$, even-L channels, which according to Eq. (9) are composite. Here we use the supermultiplet approximation and identify the phase shifts $\delta_L^{[22]}$ with the known phase shifts ${}_S\delta_L$, $S=2$, as noted above. Then from (9) we can determine the "experimental" values of the phase shifts $\delta_L^{[4]}$. However, we must take into account a new feature: the possible nonunitarity of the elastic $S=0$, even-L channels, reflected by Eq. (8). After all, if $\eta_L \ll 1$, the phase-shift analysis is meaningless, as it becomes unstable.

Direct information on η_L could be obtained by experimental study of the four-particle disintegration $dd_s\to dd_s$ with the detection of the two final protons in an interval of at least $\Delta E\cong 10$ MeV from threshold, taking into account the charge-exchange channels (10), $d+d\to np+np$ and $pp+nn$. However, these very important data are not yet available. This cross section should be small compared with that for the elastic process, since the cross section in a channel with given S contains the statistical factor $(2S+1)$ (Ref. 33), and, on the whole, channels with total spin $S=2$ dominate, while channels with $S=1$ also play a significant role.

Let us consider this question of the inelasticity in our potential model, for which we construct the potential $V^{[4]}(r)$ satisfying the following requirements. It must give binding energies of the dd system close to the experimental values $\varepsilon(0_1^+)=-23.8$ MeV and $\varepsilon(0_2^+)=-3.7$ MeV, while not leading to a $2^+(NL=22)$ bound state. It should give it in agreement with the available experimental indications[41] in the form of a resonance at 2–5 MeV [for the $\alpha\alpha$ system the $2^+(NL=42)$ level is located 2.8 MeV above the $0^+(NL=40)$ level; Refs. 4, 26, and 27]. All these requirements in the form of a (perhaps not optimal) compromise are satisfied by the potential with parameters

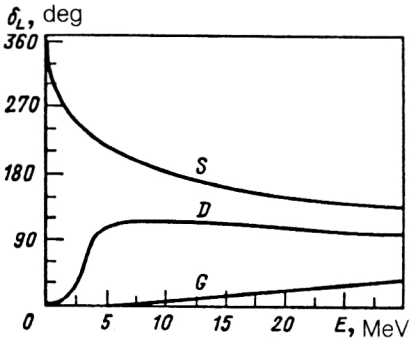

FIG. 4. Phase shifts for the potential $V^{[4]}(r)$. The experimental data are not reproduced (see the text).

$$[f]=[41],\quad V_0=-70.0\ \text{MeV},$$
$$R_0=1.92\ \text{F},\quad a=0.95\ \text{F}, \tag{14}$$

the phase shifts for which are shown in Fig. 4. The energies of the 0_1^+ and 0_2^+ levels are, respectively, $\varepsilon=-24.0$ and -0.5 MeV (the Coulomb interaction is included everywhere).

Using the phase shifts $\delta_0^{[4]}(E)$ and $\delta_2^{[4]}(E)$ that we have obtained together with the phase shifts $\delta_0^{[22]}(E)$ and $\delta_2^{[22]}(E)$ discussed above, from Eq. (8) we directly obtain $\eta_L\ll 1$ for $l=0$ and 2 right in the region of the experimentally measured phase shifts $E_{\text{c.m.}}=6$–7 MeV. Of course, Eq. (9) is literally valid at energies considerably above the $dd\to dd$ threshold, but qualitatively it suggests an interesting phenomenon even closer to the threshold. Therefore, on the one hand, it would be important to experimentally observe the dominant inelasticity $dd_s\to dd_s$ in a region several MeV wide above the threshold for the singlet channels with $S=0$ and even L, while, on the other hand, we cannot determine the above-mentioned "experimental" phase shifts $\delta_L^{[4]}$, or verify Eq. (9), etc. It is apparently difficult to see the effect of the strong absorption in the singlet channels from the form of the differential cross section for elastic scattering because of the small contribution of the singlet channels, but in Fig. 5 we show the calculated charge-exchange cross section for the energy $E=12.65$ MeV, which assumes a coincidence measurement of the pp pair.

Of course, the entire scheme for treating $d+d$ scattering is literally applicable also to ^{6}Li+^{6}Li scattering (for example, there are obvious analogs in the multiplication of the Young schemes). In particular, there are some experimental data on spin–isospin flip[42] analogous to the data on $d+d\to d_s+d_s$. But here the supermultiplet splitting of the potentials will play a smaller relative role than in the case of the $d+d$ system.

We note that a dd potential very close to the potential (13) is optimal for describing the stripping (α,d) reaction on light nuclei by the distorted wave method[43] [this, by definition, is precisely the potential $V^{[4]}(r)$]:

$$(\alpha,d):\ V_0=-66.6\ \text{MeV},\quad R_0=2.01\ \text{F},\quad a=1.0\ \text{F}.$$

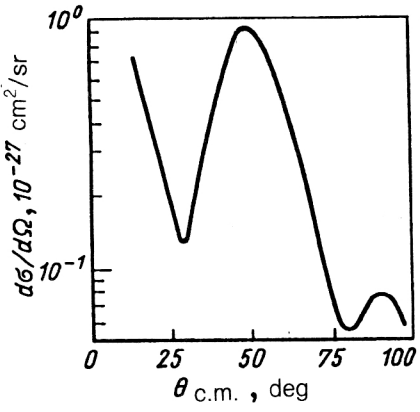

FIG. 5. Differential cross section for the reaction $d+d\to d_s+d_s$ for $E_{\text{c.m.}}=12.65$ MeV.

We also note that the potential $V^{[4]}(r)$ (13) exceeds the potential $V^{[22]}(r)$ (11) in the "strength" $V_0R_0^2$ by about 3 times, which is a beautiful manifestation of supermultiplet effects.[33] This difference is obtained immediately in the simplest numerical version of the resonating-group method, where, however, projection according to the Young schemes is applicable and effective local potentials are derived.[44] The potential $V^{[22]}(r)$ has neither bound states nor resonances (a bound S state with energy $\varepsilon\approx -6$ MeV is forbidden). Therefore, in particular, there is no bound four-neutron system corresponding to a system of two bineutrons ($[f]=[22]$, $L^\pi=0^+$, $T=2$, $S=0$, and in the supermultiplet approximation this level would be close in energy to the level with $L^\pi=0$, $T=0$, $S=2$, of which there is no hint).

Owing to the small binding energy of the forbidden S state, the S-wave node in the continuum for small positive energies lies outside the range of the potential (see Fig. 2) and therefore will be relatively mobile as the energy is changed, in contrast to the $\alpha\alpha$ system.[4,26,27]

We see that there is a very strong dependence of the interaction on the spin, not directly, but via the Young scheme $[f]$. Nevertheless, polarization effects are weak[12,16] because the J splitting of the phase shifts is small (this is determined by the weak effect of the tensor or spin–orbit forces). To refine the potential $V^{[4]}(r)$ it would be useful to have data on the photodisintegration reaction $^4\text{He}+\gamma\to d+d$ (Ref. 45), where the final state can have the Young scheme $[f]=[4]$ (quadrupole absorption sensitive to the D resonance) and $[f]=[31]$ (spin–dipole absorption with P-wave excitation and change of the total spin S). In these photonuclear data there is no interference between the amplitudes $T_L^{[4]}$ and $T_L^{[22]}$, which, as we shall see, obscures the manifestation of the potential $V^{[4]}(r)$ in dd scattering. Our simple and clear treatment will apparently be equivalent to the RGM calculation if the channel coupling $dd\leftrightarrow d_sd_s$ is included (this has not been done) and the elementary algebra of the $SU(4)$ group is used.

With the summary of Eqs. (12)–(14) and using Refs. 4, 26, and 27, we can give the systematics of the "parent" potentials $V^{[44]}(r)$, $V^{[33]}(r)$, and $V^{[22]}(r)$ for systems of identical particles successively describing $\alpha\alpha$ (even L, $S=0$), th (odd L, $S=0$), and dd (even L, $S=0$ or 2) scattering:

$$\begin{aligned}
&[f]=[44],\quad V_0=-125\ \text{MeV},\\
&R_0=1.78\ \text{F},\quad a=0.66\ \text{F},\\
&[f]=[33],\quad V_0=-76.5\ \text{MeV},\\
&R_0=1.85\ \text{F},\quad a=0.71\ \text{F},\\
&[f]=[22],\quad V_0=-41.5\ \text{MeV},\\
&R_0=1.45\ \text{F},\quad a=0.81\ \text{F}.
\end{aligned}\tag{15}$$

Here the successive deletion of a column from two squares causes the relative weight of antisymmetric pairs to systematically increase, and this in relation to the Majorana forces is the main reason for the rapid decrease of the potential "strength" $V_0R_0^2$. Actually, the strength decreases much more slowly in a different family of potentials, where the decrease of the number of nucleons in the $\alpha\alpha$–th–dd system is accompanied, conversely, by a decrease of the relative weight of antisymmetric pairs (in the th system, L is even and $S=1$; in the dd system L is even and $S=0$):

$$\begin{aligned}
&[f]=[44],\quad V_0=-125\ \text{MeV},\\
&R_0=1.78\ \text{F},\quad a=0.66\ \text{F},\\
&[f]=[42],\quad V_0=-97.5\ \text{MeV},\\
&R_0=1.85\ \text{F},\quad a=0.71\ \text{F},\\
&[f]=[4],\quad V_0=-70.0\ \text{MeV},\\
&R_0=1.92\ \text{F},\quad a=0.95\ \text{F}.
\end{aligned}\tag{16}$$

3. CONSTRUCTION OF THE POTENTIALS $V_L^{[f]}$ FOR THE $d+p$ AND $d+h$ SYSTEMS

Here we are dealing with a region which is much better studied experimentally than the region considered in the preceding section. According to the above discussion, we write

$$S_{L,S}^{\text{el}}=\eta_{L,S}\exp(2i\delta_{L,S})\equiv T_{L,S}+1,\tag{17}$$

$$\delta_{L,1/2}=\tfrac{1}{2}\delta_L^{[f_1]}+\tfrac{1}{2}\delta_L^{[f_2]},\tag{18}$$

$$\delta_{L,3/2}=\delta_L^{[f_1]},\tag{19}$$

$$\eta_{l,1/2}=|\cos(\delta_L^{[f_1]}-\delta_L^{[f_2]})|,\tag{20}$$

$$\eta_{l,3/2}=1.\tag{21}$$

The nonunitarity of the elastic scattering amplitude in the doublet channels (20) arises from the inclusion of the deuteron spin–isospin-flip channels $d+p\to d_s+p$, $d+h\to d_s+h$ and the charge-exchange channels $d+p\to pp+n$, $d+h\to pp+t$:

$$\begin{aligned}
&S_{L,1/2}^{\text{flip}}=(\tfrac{1}{2}\ \tfrac{1}{2},10|\tfrac{1}{2}\ \tfrac{1}{2})(\tfrac{1}{2}T_L^{[f_1]}-\tfrac{1}{2}T_L^{[f_2]}),\\
&S_{l,1/2}^{\text{c}}=(\tfrac{1}{2}\ \tfrac{1}{2},11|\tfrac{1}{2}\ \tfrac{1}{2})(\tfrac{1}{2}T_L^{[f_1]}-\tfrac{1}{2}T_L^{[f_2]})
\end{aligned}\tag{22}$$

[here the coefficients are the Clebsch–Gordan coefficients of the isospin group $SU(2)$]. The S matrix is unitary:

$$|S^{\rm el}_{L,1/2}|^2+|S^{\rm flip}_{L,1/2}|^2+|S^{\rm c}_{L,1/2}|^2=1, \quad |S^{\rm el}_{L,3/2}|^2=1. \tag{23}$$

Following Ref. 20, let us discuss the problem of reconstructing the potentials $V_L^{[f]}(r)$ corresponding to different allowed spatial permutation symmetries $[f]$. We begin our discussion with the $p+d$ system. For it there is a great deal of experimental data on the phase shifts and inelasticity parameters η_L in a wide range of energies up to 30 MeV and for a large set of partial waves $l=0$–8 (Refs. 46 and 47).

The experimental data on $p+d$ scattering are in good agreement with theoretical calculations carried out on the basis of solving the Faddeev equations.[48] Analyzing the experimental data, we notice the fairly large inelasticity of the doublet channels ($\eta_L\leqslant 0.5$ for $E\geqslant 7$ MeV) and the unitarity of the quartet channels ($\eta_L\cong 1$ in the entire energy range), which directly corresponds to our approach (20), (21). Furthermore, the behavior of the S- and D-wave phase shifts in the quartet channels is interesting: the D-wave phase shift is negative at low energies ($\cong -10°$) and then changes sign, and the S-wave phase shift is characterized by a sharp falloff with increasing energy. This indicates the presence of a peripheral repulsion related to nucleon exchange (the effect of such exchange has been well studied in heavy-ion reactions[11]). We construct the corresponding potentials in the form

$$V_L^{[f]}(r)=V_1\exp(-\alpha r^2)+V_2\exp(-\beta r), \tag{24}$$

where the exponential addition models the repulsion at the periphery. This conclusion, first obtained in the preliminary study of Ref. 49, has been confirmed by the independent results of Ref. 50. In constructing the potentials we take into account their splitting in the parity of the orbital angular momentum.[39]

Reconstructing the potential $V_L^{[21]}$, for even L we start from the fact that it must have a forbidden S state, since the symmetry [21] is realized beginning with the configuration $0s(1p)^2$. In the fractional-parentage decomposition of this three-nucleon configuration into the product of an $(0s)^2$ state of the deuteron and the function $\chi(r)$ of the p–d relative motion, nodal behavior (the $2S$ state) appears in the latter, owing to the conservation of the number of oscillator quanta, and the nodeless wave function $\chi(r)$ of the form $0S$, corresponding to the $(0s)^3$ configuration, is excluded by the Pauli principle (we are considering quartet channels). The corresponding deep potential $V_L^{[21]}$ for even L contains this state as a forbidden state (see Refs. 4, 26, and 27). The node of the wave function $\chi(r)$ in the S wave was interpreted earlier as a repulsive core.[26] It is interesting that in the rigorous three-particle scattering theory it is possible[51] to find an interpretation of these forbidden states as so-called ghost states.

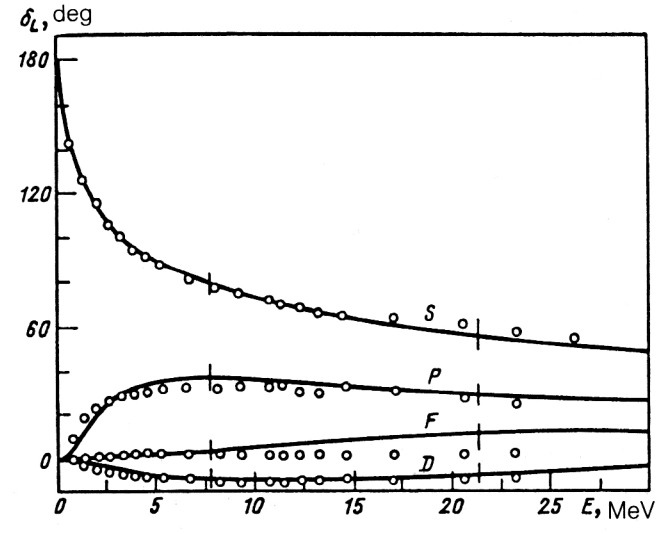

FIG. 6. Phase shifts for $p+d$ interaction potentials in channels with $[f]=[21]$ (taking into account the Coulomb interaction). The experimental values of the phase shifts are from Ref. 47, and the spread of the experimental phase-shift data of Ref. 46 is shown.

The parameters of the potential $V_L^{[21]}$ in the form of Ref. 24, reconstructed from the experimental phase shifts[47] for even L, are given in Table I. The energy of the forbidden state is $E=-2$ MeV. In Fig. 6 we show the results of calculating the phase shifts for scattering with the potential $V_L^{[21]}$ for even L, where the Coulomb interaction in the $p+d$ system is also included.

The potential $V_L^{[2]}$ for odd L does not give forbidden states. The behavior of the phase shifts[47] makes it possible to choose it to be an attractive Gaussian potential. Its parameters are given in Table I. The phase shifts for this potential, taking into account the Coulomb interaction, are given in Fig. 6.

Turning now to the nonunitary doublet channels, we note that direct reconstruction of the potentials $V_L^{[3]}$ from the experimental phase shifts is impossible, since in a $p+d$ scattering experiment states with symmetry $[f]=[3]$ are not realized in pure form. However, using the supermultiplet aproximation (18) and identifying the phase shifts $\delta_L^{[21]}$ with the quartet states, it becomes possible to isolate

TABLE I. $p+d$-interaction potentials.

$[f]$	L	V_1, MeV	α_1, F^{-2}	V_2, MeV	α_2, F^{-1}	W_1, MeV	α_1, F^{-2}	Strength
21	Even	−57,0	0,37	7,2	0,36	—	—	−53
21	Odd	−8,8	0,06	—	—	—	—	−73
3	Even	−55,8	0,31	—	—	17,0	0,43	−90
3	Odd	−13,8	0,16	1,6	0,09	−6,24	0,33	−30

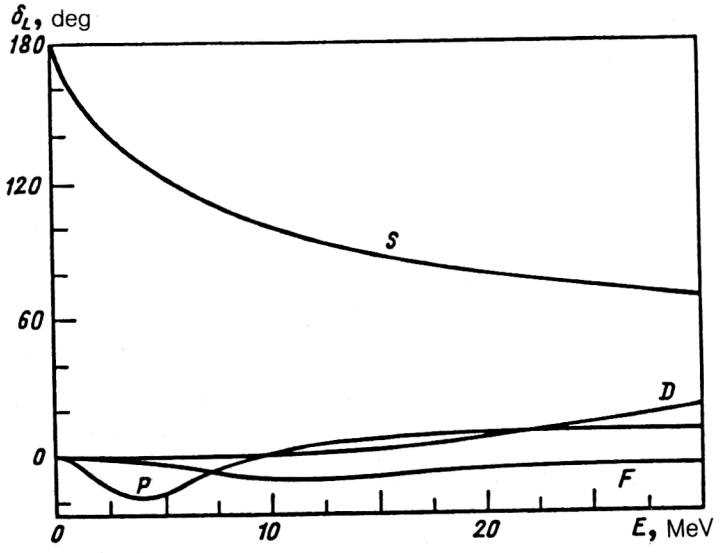

FIG. 7. Phase shifts for the $p+d$ interaction potentials in channels with $[f]=[3]$ (taking into account the Coulomb interaction).

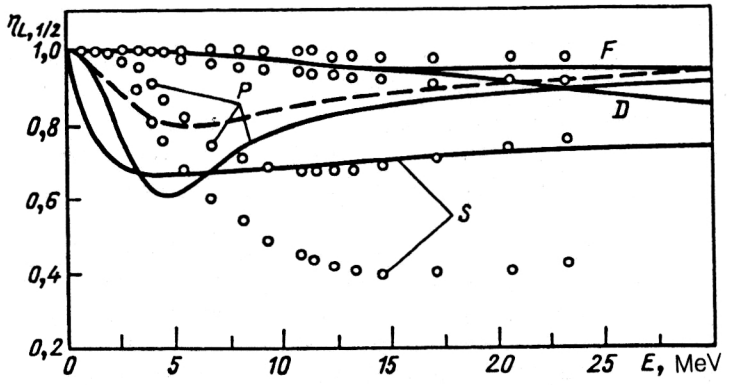

FIG. 8. Reflection coefficient $\eta_{L,1/2}$ in doublet channels ($S=1/2$) of the $p+d$ system.

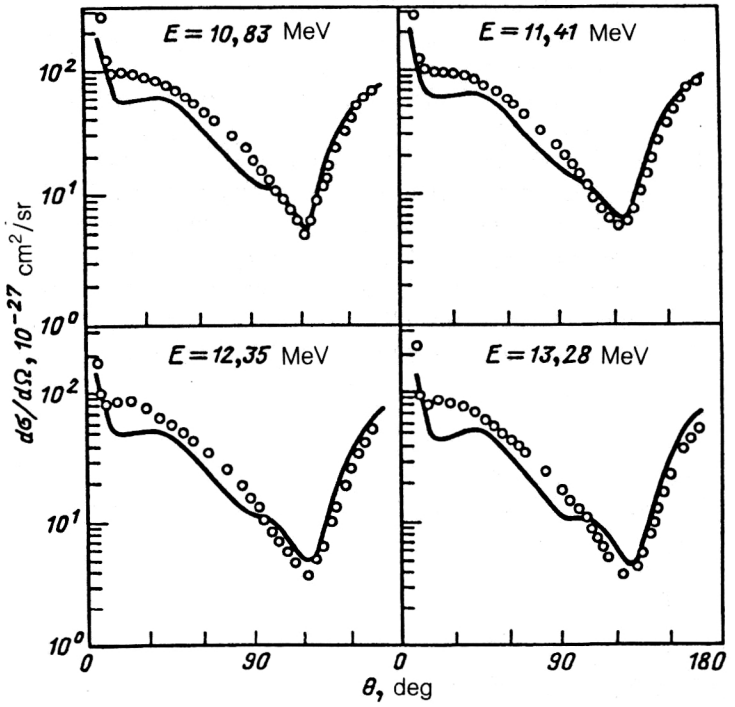

FIG. 9. Differential cross sections for elastic $p+d$ scattering for four values of the scattering energy. The experimental values of the cross sections are from Ref. 52.

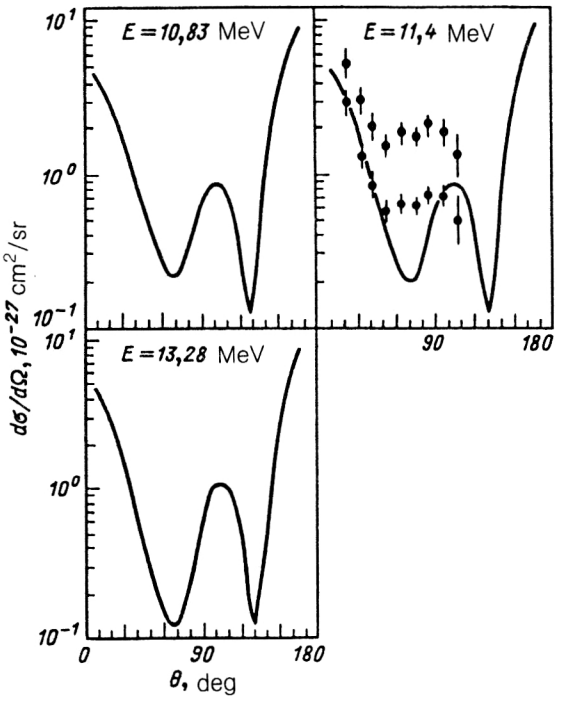

FIG. 10. Differential cross sections for the deuteron spin–isospin flip to the singlet spin state for various values of the scattering energy. The experimental values for $E=11.4$ MeV are from Ref. 53.

the "pure" phase shifts $\delta_L^{[3]}$ at energies several times above the threshold. These phase shifts should then be used to reconstruct the potentials $V_L^{[3]}$. Here we must take into account the fact that in the case of significant nonunitarity of the elastic channels with $S=\frac{1}{2}$, i.e., for $\eta_L \ll 1$, the phase-shift analysis becomes unstable. Therefore, for a reliable determination of the potentials $V_L^{[3]}$ it is necessary to use additional data, for example, the cross sections for ^{3}He photodisintegration and for $p+d$ radiative capture. The effect of triplet three-particle disintegration can be taken into account by the introduction, into the potential, of an imaginary term in the form $iV_1\exp(-\alpha_1 r^2)$.

In the reconstruction of the potential $V_L^{[3]}$ for even L it is necessary to take into account the fact that the S state in this potential is the ground state of the ^{3}He nucleus as a $p+d$ bound system with binding energy $E=5.5$ MeV. The parameters of the potentials $V_L^{[3]}$ are given in Table I, and their corresponding phase shifts are shown in Fig. 7 (with the Coulomb interaction included). In Fig. 8 we show the inelasticity parameters $\eta_{L,1/2}$ for the lowest partial waves with $L=0$–3 calculated using (20).

In Fig. 9 the differential cross sections for proton elastic scattering on the deuteron are compared with the experimental data of Ref. 52 for two values of the scattering energy. In Fig. 10 we show the differential cross sections that we calculated for deuteron spin–isospin flip into the singlet. For comparison we show the results of Ref. 53, in which the experimental values of the cross sections are normalized by two different methods. We note that the available experimental data are for an angular range which does not include the characteristic dip in the cross section near $\theta=120°$, and it is very important to make more complete measurements in this region.

We have therefore found the interaction potentials and the corresponding $p+d$ scattering amplitudes in all the allowed channels with $S=\frac{1}{2}$ and $\frac{3}{2}$, and also $[f]=[3]$ and $[f]=[21]$. The reliability and effectiveness of the potentials that we have found have been studied in Ref. 54 for the ^{3}He photodisintegration reaction $^3\mathrm{He}(\gamma,p)d$.

Let us now turn to the analysis of the $d+h$ system (Table II). Owing to the poor accuracy of the experimental data on the elastic scattering cross sections and the polarizations, the phase-shift analysis for this system was carried out only at low energies ($E\leqslant 3.4$ MeV) and turned out to be ambiguous.[55] For higher energies we make direct use of the differential cross sections for elastic scattering[56] and the phase shifts calculated in Ref. 57 by the resonating-group method.

In constructing the potential $V_L^{[32]}$ for even L we start from the fact that it must have a forbidden S state, since five-nucleon states with the Young scheme $[f]=[32]$ are realized beginning with the s^3p^2 configuration, which in the fractional parentage decomposition into states $3N\times 2N\times\chi(r)$ again gives a function for the ^{3}He and d relative motion which contains a node. The lowest observed state of positive parity is the known resonance with $J^\pi=\frac{3}{2}^+$ at $E=0.26$ MeV (Ref. 56) in the $d+h$ system. Using the quartet phase shifts calculated with the RGM (Ref. 57) as the initial approximation, we then refine the potential $V_D^{[32]}$ directly using the differential cross sections for $d+h$ elastic scattering.[56] The resulting phase shifts for channels with $S=\frac{3}{2}$, even L, and $[f]=[32]$ are shown in Fig. 11, and the potential itself is given in Table I. The energy of the forbidden state is $E=-4.61$ MeV. In the case of odd L we take into account the presence of a forbidden P state (the lowest allowed configuration is s^2p^3). The parameters of the potential $V_L^{[32]}$, again chosen to be of the form (24), for odd L are given in Table I, and the corresponding phase shifts $\delta_L^{[32]}$ are shown in Fig. 11. The energy of the forbidden state is $E=-8.0$ MeV.

TABLE II. $d+^3$He interaction potentials.

$[f]$	L	V_1, MeV	α_1, F^{-2}	V_2, MeV	α_2, F^{-1}	Strength
32	Even	−50,0	0,15	—	—	−167
32	Odd	−73,1	0,23	18,1	0,56	−123
41	Even	−57,0	0,16	8,4	0,21	−138
41	Odd	−69,0	0,14	—	—	−246

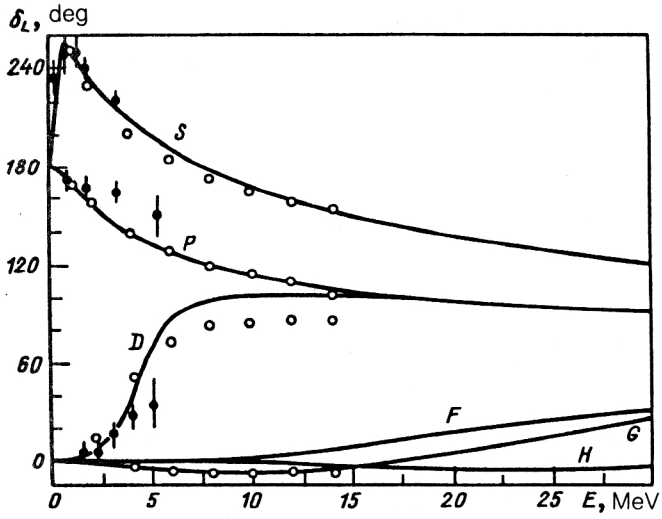

FIG. 11. Phase shifts of $d+{}^3$He scattering in the channels with $[f]=[32]$ (including the Coulomb interaction). The RGM phase shifts are from Ref. 57 (open circles), and the experimental phase shifts are from Ref. 55 (black circles).

Now let us consider nonunitary doublet channels. Using Eq. (18), we reconstruct the phase shifts $\delta_L^{[41]}$ corresponding to the Young scheme $[f]=[41]$. In reconstructing the potentials $V_L^{[41]}$ we shall start from the fact that the potential $V_L^{[41]}$ for even L contains a forbidden S state, while for odd L it contains an observed bound P state corresponding to the $J^\pi=\frac{3}{2}^-$ ground state of ^{5}Li in the $d+h$ channel. The $J^\pi=\frac{3}{2}^-$ state decays via the channel ${}^4\mathrm{He}+p$ with the large spectroscopic factor $S_p\cong 1$ (Ref. 29).

The parameters of the potentials $V_L^{[41]}$ that we found are given in Table I, and the corresponding phase shifts are shown in Fig. 12 (including the Coulomb interaction). The energy of the forbidden state of the potential $V_L^{[41]}$ for even L is $E=16$ MeV. Here we again note the large role played

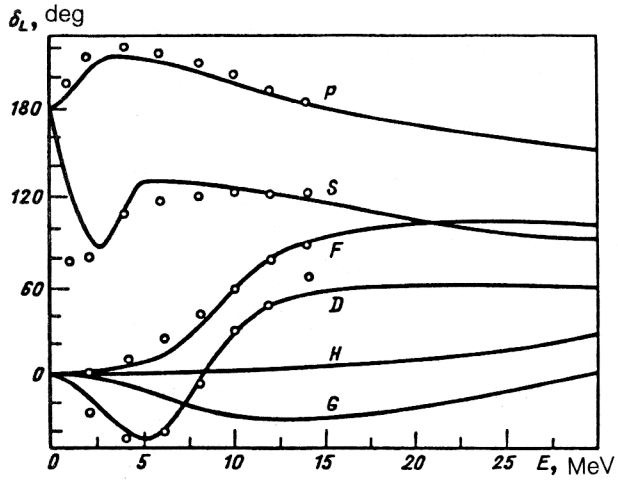

FIG. 12. Phase shifts of $d+{}^3$He scattering in the channels with $[f]=[41]$. The values of the "pure" phase shifts $\delta_L^{[44]}$ obtained from the RGM phase shifts of Ref. 57 are indicated.

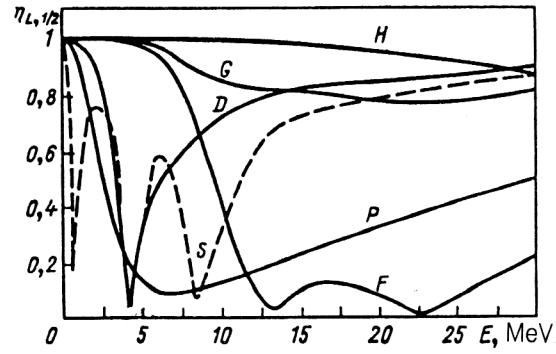

FIG. 13. Reflection coefficients $\eta_{L,1/2}$ in doublet channels of the $d+{}^3$He system.

by peripheral repulsion for even L. This is explained by the complicated behavior of the S-wave phase shift and the negative values of the D-wave phase shift at low energies. The D-wave phase shift changes sign with increasing E. Comparing the theoretical result with the phase shifts $\delta_L^{[32]}$ obtained from the RGM calculations, we note that here also $\eta_L \ll 1$ (Fig. 13) and that the inclusion of this fact in the RGM procedure via the purely phenomenological introduction of a strong imaginary part in the interaction potential does not give the coupling $dh \to d_s + ppt$. The agreement with the experimental data on the differential cross sections for elastic scattering with our values of the phase shifts is also good, as can be seen from Fig. 14. In Fig. 15 we show our predictions for the inelastic cross sections for deuteron spin–isospin flip into the singlet state, $d+h \to pp+t$, which can be measured by detecting the triton (or the pp pair). It is very desirable to carry out such an experiment.

Turning to the analysis of the potentials $V_L^{[f]}(r)$ (see Table I), we note that potentials corresponding to different spatial symmetries $[f]$ differ strongly in strength, even for the same system. It is convenient to define the strength by the volume integral

$$w_L^{[f]}(r) = \int V_L^{[f]}(r) r dr. \tag{25}$$

This strength is decreased considerably in going from states with a more symmetric Young scheme $[f]$ to states with a less symmetric scheme, owing to which the scattering amplitudes for different $[f]$ differ strongly. This fact justifies the use of the supermultiplet scheme, in spite of its approximate nature.

Our results allow us to understand why the attempt to construct a potential description of the doublet channels in the $d+p$ system with the single potential $V_{L,1/2}$ (Ref. 21) encountered serious difficulties.

4. INTERACTION OF THE *pt* AND *ph* CLUSTERS

In the case of proton elastic scattering on ^{3}He, we have $[f_A]=[1]$, $t_A=\frac{1}{2}$, $\tau_A=\frac{1}{2}$, $S_A=\frac{1}{2}$ and $[f_B]\equiv[3]$, $t_B=\frac{1}{2}$, $\tau_B=\frac{1}{2}$, $S_B=\frac{1}{2}$. The total isospin of the system is $t=1$, and the allowed values of $[f]$ are determined by the outer product

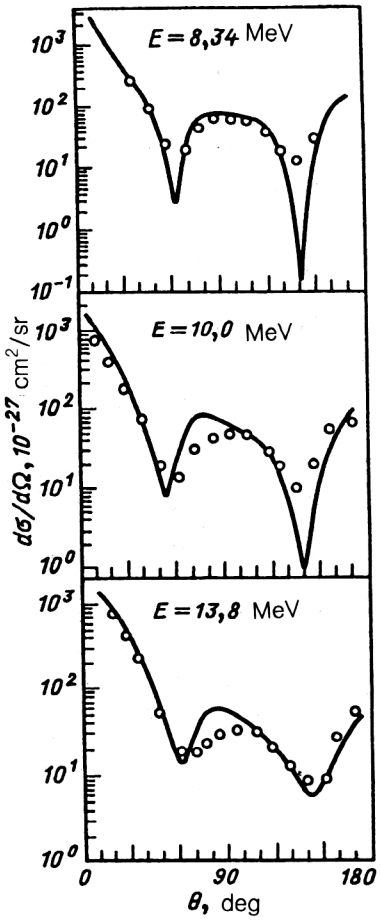

FIG. 14. Differential cross sections for elastic $d+{}^3$He scattering at various energies. The experimental data are from Ref. 56.

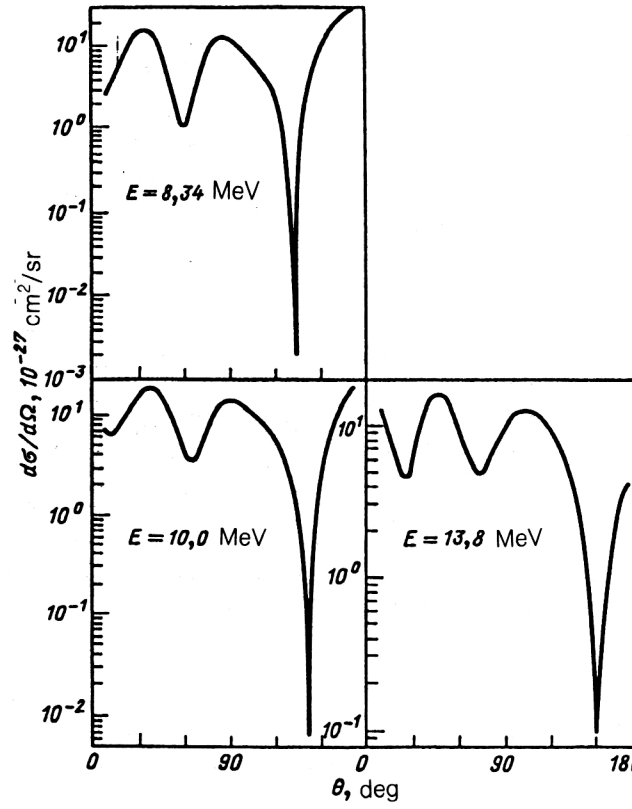

FIG. 15. Differential cross sections for the charge-exchange reaction $d+{}^3\mathrm{He}\to pp+{}^3\mathrm{H}$ for various energies.

$[1]\times[3]=[31]+[4]$. Using the values of the isoscalar factors of the group $SU(4)$ (Ref. 37), we find that in channels with $S=1$ and $S=0$ the scattering amplitude is the purely potential amplitude $T^{[31]}_{L,1,S}$. However, in the case of $p+t$ scattering we find that in singlet channels with $S=0$ the partial scattering amplitude $T_{L,S=0}$ is a superposition of potential amplitudes with different fixed Young schemes $[f]$ and total isospins t:

$$T_{L,0}=(t_p-\tau_p t_t\tau_t|00)^2T^{[4]}_{L,0,0}+(t_p\tau_p,t_t\tau_t|10)^2T^{[31]}_{L,1,0}. \tag{26}$$

The formally allowed term with $[f]=[31]$ and $t=0$ is absent, since the corresponding isoscalar factor is zero (all such factors which are nonzero are unity for our examples).

For triplet channels in the $p+t(S=1)$ system there is only isospin interference:

$$T_{L,1}=(t_p\tau_p,t_t\tau_t|00)^2T^{[31]}_{L,0,1}+(t_p\tau_p,t_t\tau_t|10)^2T^{[31]}_{L,1,1}. \tag{27}$$

Going to the partial S matrix, we write

$$T^{[f]}_{L,t,S}=S^{[f]}_{L,t,S}-1, \tag{28}$$

where the amplitudes $T^{[f]}_{L,t,S}$ are potential amplitudes (this is one of the central features of the theory[18,20]),

$$S^{[f]}_{L,t,S}=\exp[2i\delta^{[f]}_{L,t,S}], \tag{29}$$

$$S^{\mathrm{el}}_{L,S}\equiv\eta_{L,S}\exp(2i\delta_{L,S})\equiv T_{L,S}+1, \tag{30}$$

$$\delta_{L,S=0}=\tfrac{1}{2}\delta^{[4]}_{L,0,0}+\tfrac{1}{2}\delta^{[31]}_{L,1,0}, \tag{31}$$

$$\delta_{L,S=1}=\tfrac{1}{2}\delta^{[31]}_{L,0,1}+\tfrac{1}{2}\delta^{[31]}_{L,1,1}, \tag{32}$$

$$\eta_{L,s=0}=|\cos(\delta^{[4]}_{L,0,0}-\delta^{[31]}_{L,1,0})|, \tag{33}$$

$$\eta_{L,S=1}=|\cos(\delta^{[31]}_{L,0,1}-\delta^{[31]}_{L,1,1})|. \tag{34}$$

The nonunitarity of the elastic scattering amplitude (33), (34) is due to the inclusion of the charge-exchange channel $p+t\to n+h$, and the corresponding S-matrix elements are

$$S^{\mathrm{c}}_{L,S=0}=\tfrac{1}{2}T^{[4]}_{L,0,0}-\tfrac{1}{2}T^{[31]}_{L,1,0}, \tag{35}$$

$$S^{\mathrm{c}}_{L,S=1}=\tfrac{1}{2}T^{[31]}_{L,0,1}-\tfrac{1}{2}T^{[31]}_{L,1,1}. \tag{36}$$

Let us first discuss the $p+h$ interaction. Consistent experimental data are available at energies $E_p\leqslant 20$ MeV (Refs. 59–63). The RGM calculations[64] agree only qualitatively with experiment. In Ref. 65 separable potentials of the first and second rank were proposed, one for each LSt partial wave in the $p+h$ system, but the symmetry $[f]$ was not introduced; i.e., elastic scattering and charge exchange were not coupled.

In reconstructing the potential $V^{[31]}_{L,t=1,S=1}$ in triplet channels ($S=1$) for even L it is necessary to take into account the fact that it possesses a forbidden S state (the configuration $(0s)^4$ is not compatible with the symmetry

TABLE III. $p+{}^3$He interaction potentials.

$[f]$	L	S	t	V_1, MeV	α_1, F^{-2}	V_2, MeV	α_2, F^{-1}	V_{SO}, MeV	α_{SO}, F^{-2}	Strength
31	Even	1	1	— 43,2	0,26	—	—	—	—	—83
31	Odd	1	1	— 21,7	0,11	—	—	—1,54	0,11	—99
31	Even	0	1	—110,0	0,37	45,0	0,67	—	—	—59
31	Odd	0	1	— 4,8	0,05	—	—	—	—	—47

$[f]=[31]$). Our calculation indicates that the energy of this forbidden state is about -5 MeV. For the analogous reason the potential $V^{[31]}_{L,t=1,S=0}$ in singlet ($S=0$) channels for even L also possesses a forbidden S state.

The parameters of our reconstructed potentials, chosen in the form (24), are given in Table III, and the corresponding phase shifts (including the Coulomb interaction) are shown in Fig. 16. We note that the second term in the potential $V(r)$ models the peripheral repulsion associated with nucleon exchange.[49]

Let us turn to the $p+t$ interaction potentials. Here the phase shifts are known only at low energies $E\leqslant 12$ MeV (Refs. 66 and 67), and their accuracy is poor. Therefore, we make direct use of the differential cross sections for elastic scattering[67,68] and charge exchange $p+t\to n+h$ (Ref. 68), which are available in a wide energy range.

The RGM description pertains only to low energies,[69] and the agreement with experiment is qualitative. Although the potentials $V^{[f]}_{L,t,S}$ cannot be reconstructed from the phase shifts, owing to the composite nature of the observed phase shifts [see Eqs. (31) and (32)], we can use the results for the $p+h$ system, changing only the Coulomb interaction. For example, we obtain the phase shifts $\delta^{[31]}_{L,t=1,S}$ for $S=0$ and 1, and then it is easy to use these phase shifts and the experimental $p+t$ phase shifts to reconstruct the "supermultiplet" phase shifts $\delta^{[4]}_{L,t=0,S=0}$. These phase shifts are shown in Fig. 17. The parameters of the corresponding potentials are given in Table IV.

In reconstructing the potential $V^{[31]}_{L,t=0,S=1}$ for even L we took into account the fact that it has a forbidden S state. Its energy is -0.01 MeV. In constructing the potential $V^{[4]}_{L,t=0,S=0}$ for even L it is necessary to take into account the fact that its S state is the $J^\pi=0^+$ ground state of the ^{4}He nucleus[39] as a $p+t$ system with binding energy

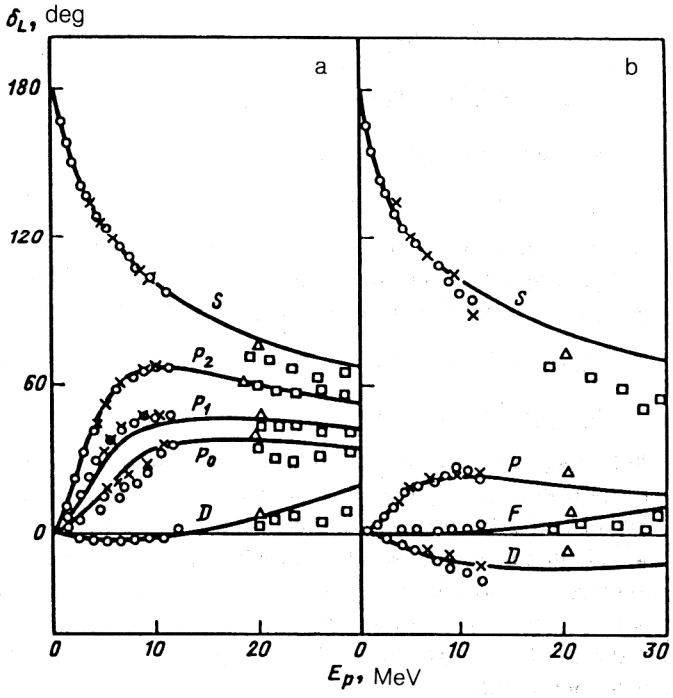

FIG. 16. Phase shifts for the potentials $V^{[31]}_{L,1,1}$ (a) and $V^{[31]}_{L,1,0}$ (b) of the $p+{}^3$He system (taking into account the Coulomb interaction). The experimental data are from the following studies: ○ from Ref. 59; × from Ref. 60; △ from Ref. 61; □ from Ref. 62.

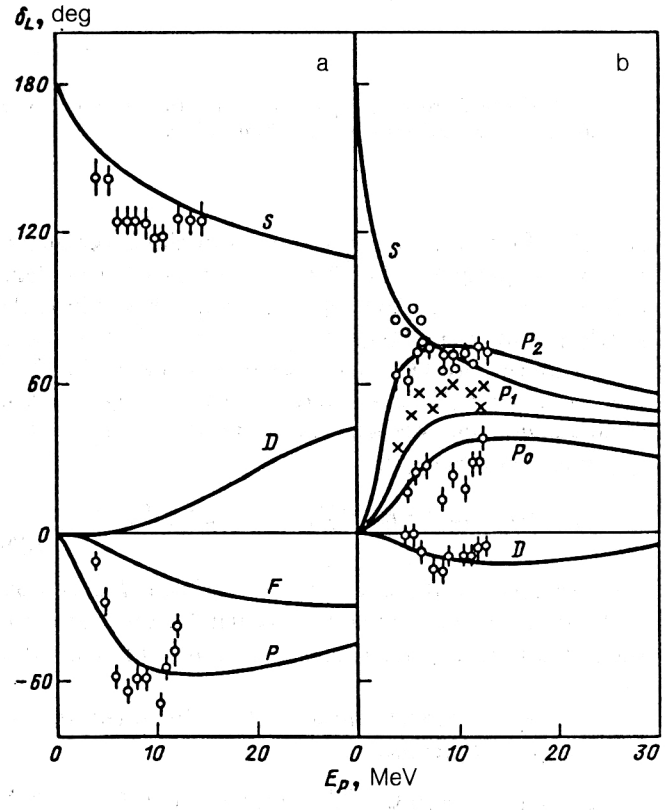

FIG. 17. Phase shifts for potentials of the $p+{}^3$H system (including the Coulomb interaction). (a) The potential $V^{[4]}_{L,0,0}$. The values of the "pure" phase shifts $\delta^{[4]}_{L,0,0}$ obtained from the experimental phase shifts[66,67] are indicated, together with the "pure" phase shifts $\delta^{[31]}_{L,0,0}$. (b) The potential $V^{[31]}_{L,0,1}$. The values of the "pure" phase shifts $\delta^{[31]}_{L,0,1}$ obtained from the experimental phase shifts[66,67] are given together with the "pure" phase shifts $\delta^{[31]}_{L,1,1}$.

TABLE IV. $p+{}^3$H interaction potentials.

[f]	L	S	t	V_1, MeV	α_1, F^{-2}	V_2, MeV	a_2, F^{-1}	V_{so}, MeV	α_{so}, F^{-2}	Strength
4	Even	0	0	−72,5	0,23	—	—	—	—	−158
4	Odd	0	0	−7,96	0,03	—	—	—	—	−133
31	Even	1	0	−47,0	0,39	6,05	0,39	—	—	−42
31	Odd	1	0	−18,2	0,11	—	—	−1,87	0,11	−83

19.8 MeV. We note that the potential that we have constructed not only reproduces the binding energy, but gives a proton momentum distribution in the ^{4}He nucleus which is in good agreement with experiment.

The differential cross sections of elastic $p+t$ scattering calculated for three values of the proton energy are shown in Fig. 18 together with the experimental cross sections, taken from Ref. 68. In Fig. 19 we show the differential cross section for the charge-exchange reaction (experiment from Ref. 68).

An important conclusion which provides justification for our approach is that the strength of the potentials (25) decreases considerably as the symmetry [f] decreases. At the same time, the additional isospin splitting of the potentials is small, but is reliably determined by the form of the charge-exchange differential cross sections.

We thus have used the generalized potential approach as a unified basis to establish for the first time a relation between the elastic-scattering and charge-exchange cross sections. In addition, the potentials obtained here can be used to obtain a quantitative description of the corresponding photonuclear reactions, as we shall show below.

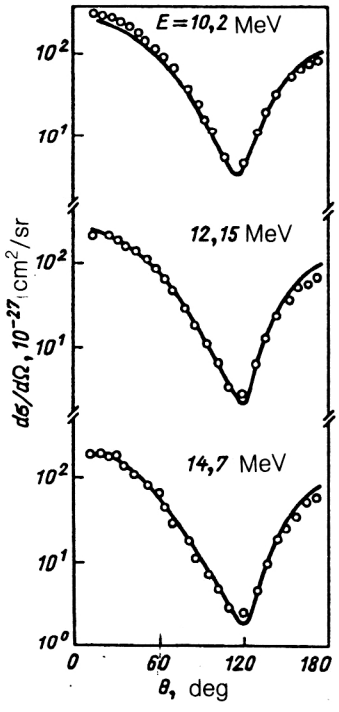

FIG. 18. Differential cross sections for $p+{}^3$H elastic scattering at various energies. The experimental data are from Ref. 68.

5. PHOTONUCLEAR REACTIONS

Beginning with the well known studies of Gorbunov,[70] photonuclear reactions involving the lightest nuclei have attracted the attention of both experimentalists[71–73] and theoreticians.[74–76] As a rule, the theoretical description of radiative capture processes and two-particle photodisintegration is based on the use of complicated multiparticle wave functions for the nuclear ground states,[77,78] or is carried out within microscopic approaches like the RGM or the K-harmonics method.[79] Although they permit certain typical features of the phenomenon to be understood, such approaches have important deficiencies. For example, the approach based on the use of multiparticle wave functions does not contain a practical recipe for including the final-state interaction for photodisintegration processes and the initial-state interaction for radiative capture processes, making it impossible to obtain an accurate quantitative description. The existing microscopic calculations (see, for example, Ref. 79) do not include the coupling of elastic scattering channels to the inelastic deuteron spin–isospin-flip and charge-exchange channels in the initial or final state, which, as shown above, plays an important role because it determines the form of the corresponding potentials and wave functions. In connection with these defects of the "accurate" microscopic approaches, the simple potential description of photonuclear reactions acquires special importance.[16,74–76] However, the traditional potential approach, which is quite adequate for describing photonu-

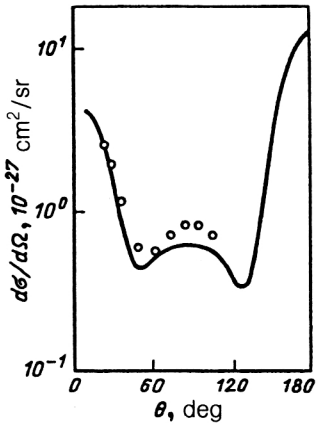

FIG. 19. Differential cross sections for the charge-exchange reaction $p+{}^3\text{H}\rightarrow n+{}^3\text{He}$ for $E=10.2$ MeV. The experimental data are from Ref. 68.

clear processes in systems characterized by a single allowed symmetry $[f]$, for example, the reactions $^6\mathrm{Li}\gamma\to d+\alpha$ and $^7\mathrm{Li}\gamma\to\alpha+{}^3\mathrm{H}$, encounters practically insurmountable difficulties when attempts are made to apply it to reactions involving very light nuclei, such as $d+d\to{}^4\mathrm{He}\gamma$ (Refs. 75 and 76). In Ref. 75 it was even concluded that this approach is inapplicable for describing photonuclear reactions involving the lightest nuclei (mainly with the specific reaction $d+d\to{}^4\mathrm{He}\gamma$ in mind). The problem here is that in systems of very light nuclei several possible spatial symmetries of the system, $[f]$, are often realized, so the traditional potential approach needs to be modified accordingly. Using the generalized potential description of nuclear interactions developed above, let us consider photonuclear reactions involving these nuclei. We will treat the problem from two viewpoints:

(1) As a good check of the cluster–cluster and nucleon–cluster interaction potentials constructed from the scattering data, especially off the mass shell.

(2) As an attempt to construct a quantitatively accurate and at the same time technically simple formalism for describing photonuclear reactions in systems of very light nuclei.

The approach proposed here is to a certain degree similar to that used in Ref. 80 to study the electromagnetic form factors of ^{6}Li in the antisymmetrized multicluster dynamical model with Pauli projection. The characteristic feature of the approach distinguishing it from the RGM is its "antisymmetrization after variation." This amounts to first solving the dynamical problem without explicit antisymmetrization of the wave function of the system (but taking into account its effective form in terms of model interaction potentials and the conditions of orthogonality of the wave function to the forbidden states of these model potentials). Only later in the calculation of the matrix elements for electromagnetic transitions is the complete antisymmetrization of the wave functions of the final and initial states implemented. This procedure is considerably clearer and simpler than the RGM scheme. In addition, for the first time it allows a simultaneous correct quantitative description of both the scattering of very light nuclei and the photonuclear processes involving them in a wide energy range, from values slightly above the threshold to $E_\gamma=30$–40 MeV.

We shall describe photonuclear reactions involving very light nuclei using the standard formalism described in Refs. 81–85. Following Ref. 81, we write the differential cross section for two-particle photodisintegration of the ^{3}He nucleus, averaged over the projections M_J of the nuclear total angular momentum J and the photon polarizations $\lambda=\pm1$, and summed over the spin states of the final particles σ'_A and σ'_B (for reactions with unpolarized particles and photons), in the form

$$\frac{d\sigma}{d\Omega}(\vartheta)=\frac{\mu p_0}{4\pi k_\gamma}\frac{1}{2J+1}\sum_{\sigma'_A,\sigma'_B\lambda,M_J}|\langle f|\hat{O}|i\rangle|^2, \tag{37}$$

where μ is the reduced mass of the final particles A and B (the proton and deuteron), p_0 is their momentum in the c.m. frame, and $\mathbf{k}_\gamma$ is the photon wave vector.

We calculate the matrix elements $\langle f|\hat{O}|i\rangle$ of the electromagnetic interaction operator $\hat{O}$ in the long-wavelength approximation, since at the photon energies of interest to us, $E_\gamma\leqslant30$–40 MeV, the wavelength is considerably larger than the characteristic dimensions of the ^{3}He nucleus. To simplify the notation in the multipole expansion of the operator $\hat{O}$, we choose the z axis of the coordinate system to lie along the direction of the photon wave vector $\mathbf{k}$. Then

$$\langle f|\hat{O}|i\rangle=-\sum_{L,\lambda}\sqrt{2\pi(2L+1)}i^L\langle f|(\lambda\hat{T}^M_{L\lambda}+\hat{T}^E_{L\lambda})|i\rangle, \tag{38}$$

where $\hat{T}^E_{L\lambda}$ is the electric and $\hat{T}^M_{L\lambda}$ is the magnetic multipole operator. In the rest of the calculations we include only the convective part in the electric multipole operator, while in the magnetic multipole operator we include only the spin part, so that the contributions of the spin part to $\hat{T}^E_{L\lambda}$ and of the convective part to $\hat{T}^M_{L\lambda}$ are considerably smaller than them.

Of all the possible multipole transitions inducing photodisintegration of the ^{3}He nucleus, we include only the $E1$ and $E2$ and the magnetic $M1$ transitions (it follows from the experimental data of Ref. 70 that in the region $E_\gamma\leqslant30$ MeV the contribution of these transitions is dominant). The operators corresponding to these transitions have the form

$$\hat{T}^{E1}_{1\lambda}=-\sqrt{2/3}k_\gamma\sum_{j=1}^{3}\hat{e}_j r_j Y_{1\lambda}(\Omega_{r_j}), \tag{39}$$

$$\hat{T}^{E2}_{2\lambda}=-\frac{1}{5\sqrt{6}}k_\gamma^2\sum_{j=1}^{3}\hat{e}_j r_j^2 Y_{2\lambda}(\Omega_{r_j}), \tag{40}$$

$$\hat{T}^{M1}_{1\lambda}=-\frac{1}{2\sqrt{6\pi}M}k_\gamma i\sum_{j=1}^{3}\hat{\mu}_j\sigma_{j\lambda}. \tag{41}$$

We write the expressions for the electric multipole operators (39) and (40) in the form prescribed by the Siegert theorem,[86] which allows the effective inclusion of a large part of the meson exchange currents.[81]

For the wave function of the ground state of the ^{3}He nucleus we use the cluster wave function of the nucleus as a $p+d$ system:

$$|i\rangle=\{\varphi(23)\chi_{00}(R)Y_{00}(\Omega_R)\}^{[3]}|[\tilde{3}]\tfrac{1}{2}\sigma\tfrac{1}{2}\tfrac{1}{2}\rangle. \tag{42}$$

The curly brackets in (42) imply symmetrization of the spatial part of the nuclear wave function, corresponding to the spatial symmetry of the system $[f]=[3]$, $|[\tilde{f}]S\sigma tr\rangle$ is the spin–isospin function of the nucleus, $\varphi(23)$ is the (spatial) wave function of the deuteron formed by the nucleons with numbers $j=2$ and 3. For the deuteron function we use the very simple single-Gaussian parametrization:[22]

$$\varphi(23)=\left[\frac{a}{\pi}\right]^{3/4}\exp\left(-\frac{1}{2}ar_{23}^2\right),\quad \alpha=0.154\ \mathrm{F}^{-2}, \tag{43}$$

although if necessary we can also use a realistic deuteron function in the form of an expansion in a sum of several

Gaussians (this leaves the entire formalism practically unchanged). The function for the relative motion of the proton and deuteron $\chi_{00}(R)$, is an eigenfunction of the Hamiltonian

$$H^{[3]}=T+V^{[3]}_{\text{even }L}, \tag{44}$$

where $V^{[3]}_{\text{even }L}$ is the potential constructed from the scattering data in Sec. 3. It corresponds to the $J^{\pi}=\frac{1}{2}^{+}$ bound state of this potential and is found by means of a variational calculation in the form of an expansion in 15 Gaussians:

$$\chi_{00}(R)=\sum_{k=1}^{15} c_k \exp(-a_k R^2). \tag{45}$$

The symmetrization in (42) is carried out by using the Young projection operator in the nonstandard basis corresponding to the reduction $U(3)\supset U(2)\times U(1)$ (Ref. 23):

$$P^{[3]}_{[1][2];[1][2]}=\tfrac{1}{3}(E+P_{12}+P_{13}). \tag{46}$$

In the symmetrization of the spatial part of the wave function for the ground state of the ^{3}He nucleus the normalization of the function is changed, and this must be taken into account in calculating the photodisintegration cross section [Eq. (37) was derived by assuming that the initial-state wave function $|i\rangle$ is normalized to unity, while the final-state wave function $|j\rangle$ is normalized to $(2\pi)^3\sigma(\mathbf{p}_0-\mathbf{p}_0')$]. It is easy to calculate the normalization constant of the symmetrized wave function (38) directly, using the expansion (45):

$$\begin{aligned}(N^{[3]})^2=&\frac{1}{3}N^2_{\text{before}}+\frac{2^9}{9\pi}(\alpha\pi)^{3/2}\sum_{k,k'=1}^{15}c_k c_{k'}\\ &\times\Big\{[(10\alpha+9a_{k'})(2\alpha+a_{k'}+4a_k)\\ &-(3a_k-2\alpha)^2]^{-3/2}+\frac{1}{2}[(4\alpha+a_{k'}+a_k)\\ &\times(4\alpha+9(a_k+a_{k'}))-9(a_{k'}-a_k)^2]^{-3/2}\Big\},\end{aligned} \tag{47}$$

where N^2_{before} is the normalization constant of the wave function $|i\rangle$ before symmetrization (N^2_{before} is the spectroscopic factor).

The asymptote of the wave function of the continuous spectrum of the $p+d$ system in the final state corresponds to a converging wave.[87] Its partial-wave expansion has the form

$$\begin{aligned}|f\rangle\equiv\psi^{(-)}_{\mathbf{p}_0}=&4\pi\sum_{lm}\mathrm{i}^l\exp(-\mathrm{i}\delta_l)\,Y^*_{lm}(\Omega_{p_0})\\ &\times Y_{lm}(\Omega_R)\chi_{nl}(p_0R)\varphi(23)\\ &\times\left|[\tilde{1}]\frac{1}{2}\sigma'_A\frac{1}{2}\frac{1}{2}\right\rangle|[\tilde{2}]1\sigma'_B00\rangle.\end{aligned} \tag{48}$$

In this form the function $\psi^{(-)}_{\mathbf{p}_0}$ is not antisymmetric under all possible nucleon permutations. In order to obtain the completely antisymmetric wave function from (48), it is necessary to perform two operations. First, the spatial part of the wave function (48) must be symmetrized by using the projection operators (46) and

$$P^{[21]}_{[1][2];[1][2]}=\tfrac{1}{3}(2E-P_{12}-P_{13}). \tag{49}$$

Second, the spin–isospin part of the function (48) must be given a definite spin–isospin symmetry $[\tilde{f}]$ which is conjugate to the symmetry $[f]$ of the spatial part of the wave function:

$$\begin{aligned}&\left|[\tilde{1}]\frac{1}{2}\sigma'_A\frac{1}{2}\frac{1}{2}\right\rangle|[\tilde{2}]1\sigma'_B00\rangle\\ &=\sum_{s,\sigma,t,[f]}\left\langle[\tilde{1}]\frac{1}{2}\frac{1}{2},[\tilde{2}]10|[\tilde{f}]St\right\rangle\left(\frac{1}{2}\sigma'_A,1\sigma'_B|S\sigma\right)\\ &\times\left(\frac{1}{2}\frac{1}{2},00|t\tau\right)\\ &\times\left|[\tilde{1}]\frac{1}{2}\sigma'_A\frac{1}{2}\frac{1}{2};[\tilde{2}]1\sigma'_B00:[\tilde{f}]S\sigma t\tau\right\rangle.\end{aligned} \tag{50}$$

Here the total isospin of the system is $t=1/2$, $\tau=1/2$, and $[f]$ can take two different values, $[f_1]=[21]$ and $[f_2]=[3]$. Then the totally antisymmetric continuum wave function takes the form

$$\begin{aligned}|f^{[f]}\rangle=&\sum_{s,\sigma,[f]}\Big\{4\pi\sum_{lm}\mathrm{i}^l\exp(-\mathrm{i}\delta_l)\\ &\times Y^*_{lm}(\Omega_{p_0})Y_{lm}(\Omega_R)\chi_{nl}(p_0R)\varphi(23)\Big\}^{[f]}\\ &\times\left\langle[\tilde{1}]\frac{1}{2}\frac{1}{2},[\tilde{2}]10|[\tilde{f}]S\frac{1}{2}\right\rangle\left(\frac{1}{2}\sigma'_A,1\sigma'_B|S\sigma\right)\\ &\times\left|[\tilde{1}]\frac{1}{2}\sigma'_A\frac{1}{2}\frac{1}{2};[\tilde{2}]1\sigma'_B00:[\tilde{f}]S\sigma\frac{1}{2}\frac{1}{2}\right\rangle.\end{aligned} \tag{51}$$

The functions $\chi_{nl}(p_0R)$ are determined by numerically solving the Schrödinger equation with the potentials $V_L^{[f]}$ constructed earlier from the elastic and inelastic scattering data. We particularly stress the fact that only the use of such "correct" (from the viewpoint of nuclear scattering) potentials makes it possible to quantitatively describe photonuclear processes involving these nuclei without any free parameters.

Since it is impossible to antisymmetrize these functions numerically, the relative-motion functions $\chi_{nl}(p_0R)$ were expanded in an analytic basis of the form

$$\chi_{nl}(R)=R^l\sum_{k=1}^{K}\xi_k(p_0)\exp[-\kappa_k(p_0)R^2] \tag{52}$$

using a Chebyshev discretization mesh for the scaling coefficients $\kappa_k(p_0)$ (Ref. 88):

$$\kappa_k(p_0)=\kappa_1(p_0)\left[\tan\left[\pi\frac{2k-1}{4k}\right]\right]^{Q},\quad k=1,2,\ldots,K. \tag{53}$$

Here K is the number of Gaussians in the expansion (52) (the dimension of the basis), and the quantities Q and $\kappa_1(p_0)$ are selected on the basis of the condition that the

norm $|\chi_{nl}(p_0R) - \chi_{nl}^{\text{appr}}|$ be a minimum. The Chebyshev mesh (53) proved to be quite economical in the sense that a small number of basis Gaussians are needed for an "accurate" approximation of a large class of wave functions (error in the approximation of the function not exceeding 0.1%). If the approximation region is finite, the asymptotic behavior of the wave functions in question is not important. However, we note that outside the approximation region the constructed expansion χ_{nl}^{appr} of the exact wave function $\chi_{nl}(p_0R)$ can have behavior completely different from that of the true function $\chi_{nl}(p_0R)$ (for example, it can grow without bound). Therefore, in the calculation of electromagnetic transitions with high multipole order (beginning with $E2$) the requirements on the accuracy of the expansion (52) at large R and on the correct choice of the expansion length increase sharply. In the actual calculations the required accuracy in calculating the matrix elements $\langle f|\hat{O}|i\rangle$ was ensured by choosing the approximation region for the functions $\chi_{nl}(p_0R)$ and $\chi_{00}(R)$ to be fairly large: $0 \leqslant R \leqslant 20$ F.

As in the case of the initial-state function (42), the normalization of the continuum function (48) changes upon symmetrization. Since this wave function is normalized according to its asymptotic value,[87] it is necessary to determine the asymptotic form of the functions $|f^{[3]}\rangle$ and $|f^{[21]}\rangle$. For the symmetry $[f]=[3]$ in the final state (we consider only the spatial part of the wave function),

$$
\begin{aligned}
&P^{[3]}_{[1][2];[1][2]}\chi_{nl}(p_0R)\,Y_{lm}(\Omega_R)\varphi(23)\\
&\quad=\tfrac{1}{3}\{\chi_{nl}(p_0R)\,Y_{lm}(\Omega_R)\varphi(23)\\
&\qquad+\chi_{nl}(p_0R')\,Y_{lm}(\Omega_{R'}\varphi(13)\\
&\qquad+\chi_{nl}(p_0R'')\,Y_{lm}(\Omega R'')\varphi(21)\},
\end{aligned}
\tag{54}
$$

where

$$
\begin{aligned}
&\mathbf{R}'=-\tfrac{3}{4}\mathbf{r}_{23}-\tfrac{1}{2}\mathbf{R},\quad \mathbf{R}''=\tfrac{3}{4}\mathbf{r}_{23}-\tfrac{1}{2}\mathbf{R},\\
&\mathbf{r}_{13}=\tfrac{1}{2}\mathbf{r}_{23}-\mathbf{R},\quad \mathbf{r}_{21}=\tfrac{1}{2}\mathbf{r}_{23}+\mathbf{R}.
\end{aligned}
\tag{55}
$$

For $R\to\infty$ the functions $\varphi(21)$ and $\varphi(31)$ fall off, since φ is the bounded deuteron wave function (43). Accordingly, we obtain the normalized final-state wave function $|f^{[3]}\rangle$ by multiplying the function $P^{[3]}_{[1][2];[1][2]}|f\rangle$ by the normalization factor equal to the inverse coefficient of the unit operator in the projector (46). In the case of the symmetry $[f]=[3]$ this factor is 3, while for $[f]=[21]$ it is 3/2.

The calculation of the matrix elements of the electromagnetic transition operators (39)–(41) between the antisymmetrized wave functions (42) and (48) can be reduced, thanks to the Gaussian expansions (45) and (52), to elementary integrals by simple algebraic transformations (the $E1$ transition is studied in detail in the Appendix) performed using programs written in REDUCE, a language for analytic computations. Here in the operators (39)–(41) it is necessary to transform from single-particle coordinates to Jacobi coordinates, on which the cluster wave functions of the initial and final states depend. As an example, let us consider the $E2$ transition operator acting in the system

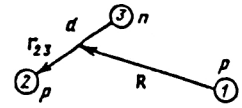

Here we have chosen the set of Jacobi coordinates $\mathbf{r}_{23}$ and $\mathbf{R}$. The $E2$ transition operator in these coordinates has the form

$$
\begin{aligned}
\hat{T}^{E2}_{2\lambda}=-\frac{1}{5\sqrt{6}}k_\gamma^2 e\Big\{&\frac{5}{9}R^2Y_{2\lambda}(\Omega_R)+\frac{1}{4}r_{23}^2Y_{2\lambda}(\Omega_{r_{23}})\\
&+\frac{1}{3}\frac{\sqrt{10\pi}}{3}\sum_{M=-1}^{1}(1\lambda-M,1M|2\lambda)\\
&\times Rr_{23}Y_{1M}(\Omega_R)Y_{1\lambda-M}(\Omega_{r_{23}})\Big\}.
\end{aligned}
\tag{56}
$$

Usually, in calculations of the photodisintegration of light and very light nuclei, the unit term proportional to R^2 is kept in this operator:

$$
\hat{T}^{E2}_{2\lambda}=-\frac{1}{9\sqrt{6}}k_\gamma^2 eR^2Y_{2\lambda}(\Omega_R),
\tag{57}
$$

since it is argued that the contribution of this term is overwhelmingly large compared with that of the other terms in (56).[89,90] A similar argument for the reasonableness of this step is given in Ref. 91. In the calculation of the differential cross section for photodisintegration of the ^{3}He nucleus to the $p+d$ channel we use the full form of the electric-dipole transition operator, including all possible Jacobi coordinates, while keeping only the part (57) dominant in the intercluster coordinate R in the electric-quadrupole transition operator. The calculations show that also in the $E1$ transition operator the dominant contribution to the matrix element $\langle f|\hat{T}^{E1}_{1\lambda}|i^{[3]}\rangle$ comes from precisely that part of the operator which is proportional to $RY_{1\lambda}(\Omega_R)$.

The explicit form of the matrix elements of the operators (39)–(41) is

$$
\begin{aligned}
\langle f|\hat{T}^{E1}_{1\lambda}|i^{[3]}\rangle=&\frac{2\pi}{9}\sqrt{2/3}k_\gamma e\exp(i\sigma_1^{[21]})\,Y_{1\lambda}(\Omega_{p_0})\\
&\times\left(\frac{1}{2}\sigma'_A,1\sigma'_B|\frac{1}{2}\sigma\right)\sum_{k,k'}c_k^{[3]}\xi_{k'}^{[21]}\\
&\times\Big\{\mathscr{L}_4^{[21]}+\frac{2\alpha^{3/2}}{\pi^{1/2}}\Big[3\,\frac{2\alpha-3\kappa_{k'}^{[21]}}{10\alpha-9\kappa_{k'}^{[21]}}+1\Big]\\
&\times\mathscr{W}_4^{[21]}\mathscr{L}_2^{[21]}+\frac{2\alpha^{3/2}}{2\pi^{1/2}}\Big[3\\
&+\frac{2\alpha-3\kappa_{k'}^{[21]}}{10\alpha+9\kappa_{k'}^{[21]}}\Big]\mathscr{W}_4^{[21]}\mathscr{G}_2^{[21]}\Big\},
\end{aligned}
\tag{58}
$$

$$\langle f|\hat{T}^{E2}_{2\lambda}|i^{[3]}\rangle=\frac{\sqrt{2\pi}}{27\sqrt{15}}k_\gamma^2 eY_{2\lambda}(\Omega_{p_0})$$
$$\times\left(\frac{1}{2}\sigma'_A,1\sigma'_B|\frac{1}{2}\sigma\right)\sum_{k,k'}c_k^{[3]}$$
$$\times\left\{\xi_{k'}^{[21]}\exp(i\delta_2^{[21]})\left[\mathscr{Q}_6^{[21]}\right.\right.$$
$$\left.+\frac{a^{3/2}}{\pi^{1/2}}\mathscr{M}^{[21]}\right]+2\xi_{k'}^{[3]}\exp(i\delta_2^{[3]})$$
$$\left.\times\left[2\mathscr{Q}_6^{[3]}-\frac{3\alpha^{3/2}}{\pi^{1/2}}\mathscr{M}^{[3]}\right]\right\},\qquad(59)$$

$$\langle f|\hat{T}^{M1}_{1\lambda}|i^{[3]}\rangle=0.\qquad(60)$$

Here

$$\mathscr{M}^{[f]}=\frac{2}{2\alpha-3\kappa_{k'}^{[f]}}\left[\frac{8}{10\alpha+9\kappa_{k'}^{[f]}}\mathscr{Q}_0^{[f]}-\mathscr{Q}_2^{[f]}\right]$$
$$\times\left[\frac{18}{2\alpha-3\kappa_{k'}^{[f]}}\mathscr{W}_2^{[f]}-\frac{38\alpha-9\kappa_{k'}^{[f]}}{10\alpha+9\kappa_{k'}^{[f]}}\mathscr{W}_4^{[f]}\right]$$
$$+8\frac{2\alpha-3\kappa_{k'}^{[f]}}{(10\alpha+9\kappa_{k'}^{[f]})^2}\left[3\frac{2\alpha-3\kappa_{k'}^{[f]}}{10\alpha+9\kappa_{k'}^{[f]}}+2\right]$$
$$\times\mathscr{W}_6^{[f]}\mathscr{Q}_0^{[f]}+\frac{1}{3}\mathscr{W}_6^{[f]}\mathscr{Q}_2^{[f]},\qquad(61)$$

$$\mathscr{W}_q^{[f]}=\int_0^{R_{\lim}}y^q\exp\left[-\frac{1}{4}\left[2\alpha+4a_k^{[31]}+\kappa_{k'}^{[f]}\right.\right.$$
$$\left.\left.-\frac{(2\alpha-3\kappa_{k'}^{[f]})^2}{10\alpha+9\kappa_{k'}^{[f]}}\right]y^2\right]dy,\qquad(62)$$

$$\mathscr{P}_q^{[f]}=\int_0^{R_{\lim}}y^q\exp\left[-\frac{1}{16}\left[10\alpha+9\kappa_{k'}^{[f]}\right.\right.$$
$$\left.\left.-\frac{(2\alpha-3\kappa_{k'}^{[f]})^2}{2\alpha+4\alpha_k^{[3]}+\kappa_{k'}^{[f]}}\right]y^2\right]dy,\qquad(63)$$

$$\mathscr{Q}_q^{[f]}=\int_0^{r_{\lim}}y^q\exp\left[-\frac{1}{16}[10\alpha+9\kappa_{k'}^{[f]}]y^2\right]dy,\qquad(64)$$

$$\mathscr{G}_q^{[f]}=\int_0^{R_{\lim}}y^q\exp\left[-\frac{1}{4}[2\alpha+4\alpha_k^{[3]}+\kappa_{k'}^{[f]}]y^2\right]dy,\qquad(65)$$

$$\mathscr{Q}_q^{[f]}=\int_0^{R_{\lim}}y^q\exp[-(\alpha_k^{[3]}+\kappa_{k'}^{[f]})y^2]dy.\qquad(66)$$

The integration in Eqs. (62)–(66) is formally extended to infinity, but it is actually necessary to integrate only up to some limiting value $R_{\lim}$. This is related to the fact that the continuum functions are expanded in Gaussians only in a finite (not too large) range of R, outside which the behavior of the approximating series (52) is arbitrary. In particular, it can increase without bound. In practice, $R_{\lim}$ is selected on the basis of the condition that the quantities $\mathscr{W}_q^{[f]}$, $\mathscr{P}_q^{[f]}$, $\mathscr{Q}_q^{[f]}$, $\mathscr{G}_q^{[f]}$, and $\mathscr{Q}_q^{[f]}$ be stable with respect to small variations of the argument y.

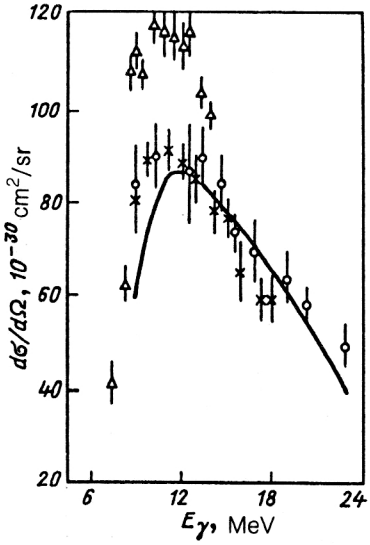

FIG. 20. Differential cross section for the reaction ^{3}He$\gamma\rightarrow p+d$ at the angle $\theta=90°$. The experimental data are from various studies: △ from Ref. 94; ○ from Ref. 96; × from Ref. 95.

It is clear from Eq. (58) that the electric dipole transition diagonal in the symmetry of the system $[f]$ does not contribute to the matrix element. The situation here is similar to that occurring in the translationally invariant shell model (TISM) in the study of transitions between bound states with different symmetries $[f]$. In fact, it is well known[23] that the transition between the states $|s^3[3]\rangle$ and $|s^2p[3]\rangle$ in the TISM is spurious. It corresponds to excitation of the center of mass of the three-nucleon system.

It is interesting to note that in the potential approach there is no magnetic dipole transition in the system. Exactly the same conclusion was drawn earlier in Refs. 92 and 93 from completely different considerations.

In Fig. 20 we show the differential cross section for the reaction ^{3}He$\gamma\rightarrow p+d$ for proton emission angle in the lab frame $\theta=90°$ in the range of photon energy E_γ from the reaction threshold $E_{\text{thr}}=5.49$ MeV to $E_\gamma=24$ MeV. This emission angle was chosen because of the availability of experimental data.[70,94–98] It should be noted that the experimentally measured cross sections for this reaction fall into two strongly differing (by up to 30%) groups (Fig. 20). The values of the photodisintegration cross sections obtained from the experimentally measured cross sections for radiative capture $p+d\rightarrow{}^3$Heγ lie considerably higher than the experimental photodisintegration cross sections obtained directly. The results of the calculation of the differential cross section for photodisintegration of the ^{3}He nucleus obtained using our generalized potential approach

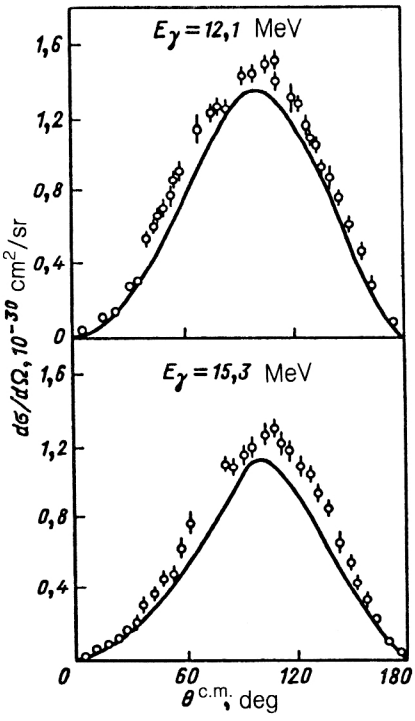

FIG. 21. Angular distributions for the reaction $p+d\to{}^3\text{He}\gamma$. The experimental points are from Ref. 99.

fall into a band lying between these two groups of experimental points.

Let us now analyze the angular distributions. We note that the overwhelming majority of experiments study the radiative capture reaction $p+d\to{}^3\text{He}\gamma$ (Refs. 94 and 99), which is the inverse of the two-particle photodisintegration of the ^{3}He nucleus. Using the detailed-balance equation,[77] we obtain the angular distributions for this reaction from (37):

$$\frac{d\sigma^{\text{capt}}}{d\Omega}(\vartheta)=\frac{2}{3}\left[\frac{k_\gamma}{k_p}\right]^2\frac{d\sigma^{\text{disint}}}{d\Omega}(\theta). \tag{67}$$

In Fig. 21 we show the results of the calculation and the experimental data of Ref. 99 for two deuteron energies, $E_d=19.8$ and 29.6 MeV. We see from this figure that the calculated results are in good agreement with experiment.

The electric dipole transition dominates in the energy range under consideration, $E_\gamma\leqslant 24$ MeV. The contribution of the $E2$ transition to the total cross section is about 2–3%, which agrees with the theoretical estimates of Refs. 100 and 101 and with the experimental results of Ref. 70. The transition itself is manifested in the angular distributions mainly through the interference with the $E1$ transition, which leads to a slight asymmetry of the angular distributions. As already noted, the $M1$ transition is absent in the potential approach (if we use the simplest model functions for the nuclei involved in the reaction). However, it follows from the experimental data (see, for example, Ref. 70) that even though the isotropic component in the angular distributions is very small, it is still there. This component owes its origin to the presence, in the ground-state wave function of the ^{3}He nucleus, of the mixed-symmetry component with $[f]=[21]$, which was not considered in our approach. We note that by including this component in the calculation of the differential cross section for ^{3}He disintegration and comparing the results with the available experimental data, we can estimate the contribution of this component to the ground-state wave function of the ^{3}He nucleus.

We conclude by pointing out another important advantage of the potential approach to the description of photonuclear reactions involving very light nuclei. This is the simple but correct inclusion of the final-state interaction. The importance of this was analyzed in Ref. 101, where it was shown that the use of the plane-wave approximation leads to an increase of 20–25% in the maximum of the differential cross section for photodisintegration of the ^{3}He nucleus to the $p+d$ channel for $\theta^{\text{lab}}=90°$.

The differential cross section for the radiative capture reaction $d+{}^3\text{He}\to{}^5\text{Li}\gamma$, averaged over the spin states of the deuteron and the helium nucleus, σ_A and σ_B, and summed over the allowed photon polarizations $\lambda=\pm 1$ and the projections M_J of the total angular momentum J of the ^{5}Li nucleus as a $d+{}^3$He system, has the form

$$\frac{d\sigma}{d\Omega}(\theta)=\frac{\mu k_\gamma}{2\pi p_0}\frac{1}{(2s_A+1)(2s_B+1)}\sum_{\sigma_A,\sigma_B,\lambda,M_J}|\langle f|\hat{O}|i\rangle|^2. \tag{68}$$

Here p_0 is the momentum of the relative motion of the deuteron and the helium nucleus in the c.m. frame in the initial state, μ is the reduced mass of these particles, and $\mathbf{k}_\gamma$ is the photon wave vector.

As in the calculation of the photodisintegration of the ^{3}He nucleus to the $p+d$ channel, we carry out all the calculations in the long-wavelength approximation (38), taking into account only the $E1$, $E2$, and $M1$ transitions (39)–(41), which give the largest contribution to the cross section (68).

As the initial-state wave function we use the continuum cluster wave function of the $d+{}^3$He system, whose asymptote is a diverging wave.[87] Its partial-wave expansion has the form

$$\begin{aligned}|i\rangle\equiv\psi^{(+)}_{\mathbf{p}_0}&=4\pi\sum_{lm}i^l\exp(i\delta_l)Y^*_{lm}(\Omega_{p_0})Y_{lm}(\Omega_R)\chi_{nl}(p_0R)\varphi_A(123)\\&\times\left|[\tilde{3}]\frac{1}{2}\sigma_A\frac{1}{2}\frac{1}{2}\right\rangle\varphi_B(45)\,|\,[\tilde{2}]1\sigma_B00\rangle,\end{aligned} \tag{69}$$

where $\varphi_B(45)$ is the spatial part of the wave function (43) of the deuteron formed by the nucleons numbered 4 and 5, and $\varphi_A(123)$ is the spatial part of the wave function of the ^{3}He nucleus:[102]

$$\begin{aligned}&\varphi_A(123)=\left[\frac{2\beta^4}{\pi^2}\right]^{3/2}\exp\left[-\beta^2\left(\frac{3}{4}r_{12}^2+\rho^2\right)\right],\\&\beta=0.385\ \text{F}^{-1},\quad \mathbf{r}_{12}=\mathbf{r}_1-\mathbf{r}_2,\quad \boldsymbol{\rho}=\tfrac{1}{2}(\mathbf{r}_1+\mathbf{r}_2)-\mathbf{r}_3.\end{aligned} \tag{70}$$

To antisymmetrize the wave function (69) using the recipe described above, we use the Young projection operators in

the nonstandard basis corresponding to the reduction $U(5)\supset U(3)\times U(2)$ (Ref. 23),

$$P^{[32]}_{[3][2];[3][2]}=\tfrac{1}{12}(6E-2P_{14}-2P_{24}-2P_{34}-2P_{15}-2P_{25}-2P_{35}+P_{14}P_{25}+P_{24}P_{15}+P_{14}P_{35}+P_{34}P_{15}+P_{24}P_{35}+P_{34}P_{25}), \quad (71)$$

$$P^{[41]}_{[3][2];[3][2]}=\tfrac{1}{15}(6E+P_{14}+P_{24}+P_{34}+P_{15}=P_{25}+P_{35}-2P_{14}P_{25}-2P_{24}P_{15}-2P_{14}P_{35}-2P_{34}P_{15}-2P_{24}P_{35}-2P_{34}P_{25}), \quad (72)$$

and also the supermultiplet expansion

$$\left|[\tilde{3}]\,\frac{1}{2}\,\sigma_A\,\frac{1}{2}\,\frac{1}{2}\right\rangle|[\tilde{2}]1\sigma_B00\rangle = \sum_{s,\sigma,t,\tau,[f]}\left\langle[\tilde{3}]\,\frac{1}{2}\,\frac{1}{2},[\tilde{2}]10|[\tilde{f}]ST\right\rangle \times\left(\frac{1}{2}\,\sigma_A,1\sigma_B|S\sigma\right)\left(\frac{1}{2}\,\frac{1}{2},00|t\tau\right) \times\left|[\tilde{3}]\,\frac{1}{2}\,\sigma_A\,\frac{1}{2}\,\frac{1}{2};[\tilde{2}]1\sigma_B00:[\tilde{f}]S\sigma t\tau\right\rangle. \quad (73)$$

The final-state wave function is the function of the $J^\pi=\frac{3}{2}^-$ ground state of the ^{5}Li nucleus as a $d+^3$He bound system:[103]

$$|f^{[41]}\rangle=P^{[41]}_{[3][2];[3][2]}\varphi_A(123)\varphi_B(45)\chi_{11}(R) \times Y_{1M}(\Omega_R)|[\tilde{41}]\,\tfrac{1}{2}\sigma\tfrac{1}{2}\,\tfrac{1}{2}\rangle. \quad (74)$$

As before, it is necessary to take into account the change of the normalizations of the initial- and final-state wave functions due to their antisymmetrization. In calculating the matrix elements of the operators (39)–(41) between the cluster wave functions (69) and (74) we use the same Gaussian expansion technique as before. In the present case for $\chi_{11}(R)$ we take

$$\chi_{11}(R)=R\sum_{k=1}^{15}c_k\exp(-a_kR^2). \quad (75)$$

In the electromagnetic transition operators we include only the part which is dominant in the intercluster coordinate R.

In Fig. 22 we show the angular distributions for the reaction $d+^3$He$\to^5$Liγ corresponding to three values of the ^{5}Li excitation energy, $E_x=E_\gamma+Q=19.9$, 20.7, and 23.2 MeV. Here $Q\approx16.6$ MeV is the binding energy of the ^{5}Li nucleus in the $d+^3$He channel according to the data of Ref. 104. The experimental data shown in this figure are also taken from that study.

The differential cross section for the reaction $d+^3$He$\to^5$Liγ at the angle $\theta=90°$ is shown in Fig. 23 together with the experimental values of the cross sections.[89] We see from Figs. 22 and 23 that the agreement between the theoretical results and the experimental data is quite satisfactory.

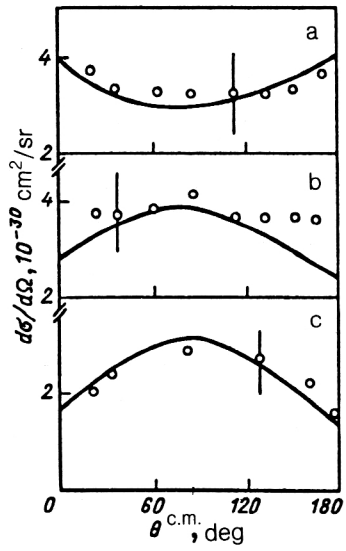

FIG. 22. Angular distributions for the reaction $d+^3$He$\to^5$Liγ. The experimental data are from Ref. 104: (a) $E_x=19.9$ MeV; (b) $E_x=20.7$ MeV; (c) $E_x=23.2$ MeV.

We note that the main contribution to the radiative-capture cross section comes from electric dipole transitions occurring with rearrangement of the spatial symmetry of the $d+^3$He system (from the state with symmetry $[f]=[32]$ to that with symmetry $[f]=[41]$). The contribution of transitions diagonal in the symmetry $[f]$ is considerably less important. Here for low energies of the final photons (see Fig. 22a) the contribution of $E1$ transitions leading to a decrease of the total angular momentum of the system J (transitions $J^\pi=\frac{3}{2}^-\to J^\pi=\frac{1}{2}^+$) is somewhat greater than the contribution of transitions leading to an increase of J (transitions $J^\pi=\frac{3}{2}^-\to J^\pi=\frac{5}{2}^+$). This is due to the presence of a clearly expressed resonance in the S wave of the potential $V^{[32]}_{\text{even }L}$. At higher energies (see Fig. 22c) the relative roles of these contributions are reversed (the transition to the $J^\pi=\frac{5}{2}^+$ resonance in the D wave of this potential plays the dominant role). The electric quadrupole transition is weaker than the electric dipole one by almost two orders of magnitude. It is manifested mainly through interference with the $E1$ transition, leading to a weak asymmetry of the angular distributions. The contribution of $M1$ transitions is negligible in this energy range.

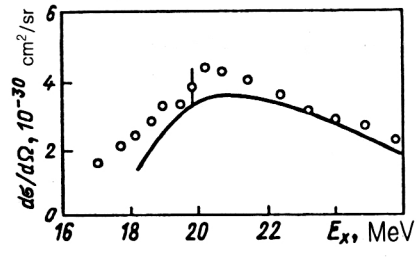

FIG. 23. Differential cross section for the reaction $d+^3$He$\to^5$Liγ at the angle $\theta=90°$. The experimental values of the cross sections are from Ref. 104.

Recently, there has been a surge of interest in the radiative capture reaction $d+d\to{}^4\mathrm{He}\gamma$ and its inverse, two-particle photodisintegration of the ^{4}He nucleus to the $d+d$ channel (Refs. 71, 73–76, 105, and 106). This is due to the possibility of determining in a relatively simple manner the admixture of the D-wave component in the ground-state wave function of the ^{4}He nucleus. In fact, in contrast to photonuclear reactions in the systems $n+{}^3\mathrm{He}$ and $p+{}^3\mathrm{H}$, where the full series of $E1$, $E2$, and $M1$ electromagnetic transitions is possible and it is necessary to take into account the complex realistic function of the three-particle nucleus (^{3}H or ^{3}He), here in an energy range not too close to the threshold at $E=23.848$ MeV and not exceeding 50 MeV, the dominant transition is the electric quadrupole transition (in the photodisintegration reaction ${}^4\mathrm{He}\gamma\to d+d$ this is the transition from the $^1S_0$ state of the ^{4}He nucleus to the $^1D_2$ scattering state in the $d+d$ system). When the admixture of the D component in the ^{4}He wave function is taken into account, another electric quadrupole transition becomes possible: for the photodisintegration process this is the transition from the $^1D_0$ state to the $^5S_2$ scattering state of the $d+d$ system. In addition, the realistic deuteron wave function is fairly well known.[107] By calculating the theoretical cross section for two-particle photodisintegration of the ^{4}He nucleus, or, nearly the same, for radiative capture $d+d\to{}^4\mathrm{He}\gamma$, and comparing the result with the available experimental data (Refs. 71, 73, 75, 76, and 108), we can extract information about the unknown admixture of the D-wave component. Here it better to avoid energies near the threshold, since there the contribution of the $M2$ transition is large, amounting to 25.3% at $E=24.448$ MeV, according to the data of Ref. 73. Our goal here is not to determine the admixture of the D component in the ground-state wave function of the ^{4}He nucleus. It is to develop a simple and effective, but also fairly accurate, formalism for calculating the cross sections of the photonuclear reactions discussed above.

As in the case of the systems considered above, we use the generalized potential approach for describing the two-particle photodisintegration of the ^{4}He nucleus. In this approach the differential cross section of the process is given by Eq. (37), where $J=0$ is the total angular momentum of the α particle. For the reasons stated above, we restrict ourselves to the inclusion of only the dominant $E2$ transition from the $^1S_0$ bound state to the continuum of the $^1D_2$ $d+d$ system (this condition imposes a certain limit on the allowed energy interval: we must not get too close to the reaction threshold, where the contribution of $M2$ transitions is large). In the electric-quadrupole transition operator (40) we transform to Jacobi coordinates

and

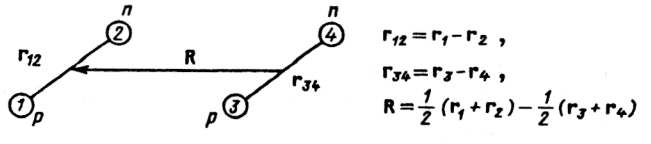

$$\hat{T}^{E2}_{2\lambda}=-\frac{k_\gamma^2 e}{5\sqrt{6}}\left\{\frac{1}{2}R^2Y_{2\lambda}(\Omega_R)+\frac{1}{4}r_{12}^2Y_{2\lambda}(\Omega_{r_{12}})+\frac{1}{4}r_{34}^2Y_{2\lambda}(\Omega_{r_{34}})+\frac{1}{2}\sqrt{10\pi/3}R\times\sum_{M=-1}^{1}(1\lambda-M,1M|2\lambda)Y_{1\lambda-M}(\Omega_R)\times[r_{12}Y_{1\lambda}(\Omega_{r_{12}})-r_{34}Y_{1\lambda}(\Omega_{r_{34}})]\right\} \tag{76}$$

and then we take into account only the leading term in the coordinate R:

$$\hat{T}^{E2}_{2\lambda}=-\frac{k_\gamma^2 e}{10\sqrt{6}}R^2Y_{2\lambda}(\Omega_R). \tag{77}$$

As the wave function of the ground state of the ^{4}He nucleus we use the cluster wave function of this nucleus as a $d+d$ system:

$$|i\rangle=\{\varphi(12)\varphi(34)\chi_{00}(R)\,Y_{00}(\Omega_R)\}^{[4]}|[\widetilde{4}]0000\rangle. \tag{78}$$

Symmetrization, denoted by the curly brackets in (78), is accomplished by means of the Young projection operator in the nonstandard basis corresponding to the reduction $U(4)\supset U(2)\times U(2)$ (Ref. 23):

$$P^{[4]}_{[2][2];[2][2]}=\tfrac{1}{3}(E+P_{13}+P_{14}). \tag{79}$$

Up to an overall factor, this projection operator was constructed earlier in Ref. 44. The normalization constant of the symmetrized wave function (78) is calculated directly using the Gaussian expansion (45) for the function $\chi_{00}(R)$:

$$(N^{[4]})^2=\frac{1}{2}N^2_{\text{before}}+\frac{4\alpha^3}{9\sqrt{\pi}}\sum_{k,k'=1}^{15}c_kc_{k'}\{4(\alpha+a_k)^{-3/2}\times[(3\alpha+a_{k'})^2-(a_{k'}-\alpha)^2]^{-3/2}+(2\alpha)^{-3/2}\times[(2\alpha+a_{k'}+a_k)^2-(a_{k'}-a_k)^2]^{-3/2}\}, \tag{80}$$

where N^2_{before} is the normalization constant of the wave function $|i\rangle$ before symmetrization.

The continuum wave function of the $d+d$ system in the final state corresponds to a converging wave in the asymptotic region.[87] Its partial-wave expansion has the form

$$|f^{[f]}\rangle\equiv[\psi^{(-)}_{p_0}]^{[f]}=4\pi\sum_{s',\sigma,[f]}\left\{\sum_{lm}i^l\exp(-i\delta_l)\,Y^*_{lm}(\Omega_{p_0})\times Y_{lm}(\Omega_R)\chi_{nl}(p_0R)\varphi(12)\varphi(34)\right\}^{[f]}\times\langle[\widetilde{2}]10,[\widetilde{2}]10|[\widetilde{f}]S0\rangle(1\sigma'_A,1\sigma'_B|S\sigma)|\times[\widetilde{2}]1\sigma'_A00;[\widetilde{2}]1\sigma'_B00:[\widetilde{f}]S0\sigma0\rangle. \tag{81}$$

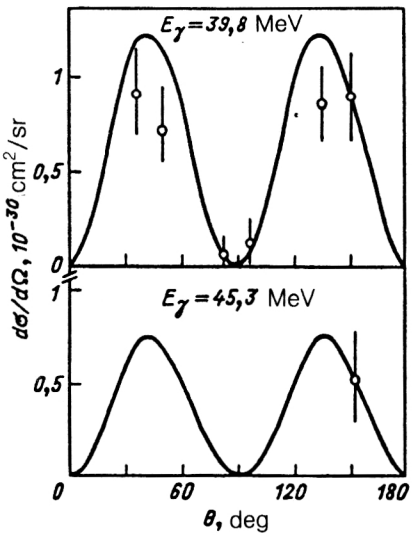

FIG. 24. Angular distributions for the reaction $\gamma^4\text{He}\to d+d$ at $E=39.8$ MeV (a) and 45.3 MeV (b). The experimental values are from Ref. 108.

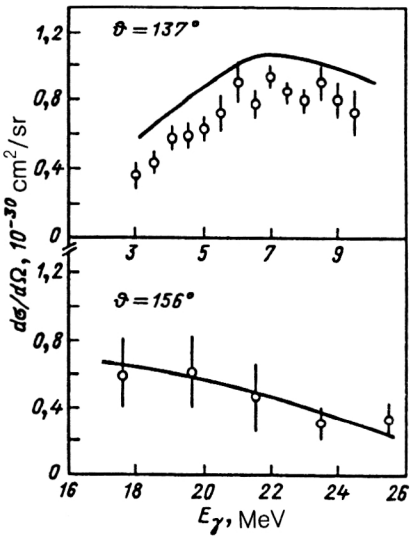

FIG. 25. Differential cross section for photodisintegration of the ^{4}He nucleus to the $d+d$ channel at $\theta=137°$ and 156° in the c.m. frame. The experimental data are from Ref. 108.

The selection rules for $[\tilde{f}]$ and S [the values of all the nonzero isoscalar factors of the Clebsch–Gordan coefficients of the group $SU(4)$] together with the requirement that the total spin S of the system be conserved give two possible final states: (1) $[f]=[4]$, $S=0$; 2) $[f]=[22]$, $S=0$. However, since the electromagnetic transition is a one-particle transition, it can lead only to a one-square rearrangement of the Young scheme of the system. For this reason only the final state 1 above is possible. Using the Gaussian expansion (52) for the function $\chi_{nl}(p_0^{\prime}R)$, we can obtain the matrix element for the $E2$ transition operator:

$$\langle f|\hat{T}^{E2}_{2\lambda}|i^{[4]}\rangle=(-1)^{1+\sigma'_A}\delta_{\sigma^*_{A'},-\sigma^*_B}\frac{k_\gamma^2 e}{9\sqrt{10}}\exp(i\delta_2^{[4]})$$
$$\times Y_{2\lambda}(\Omega_{p_0})\sum_{k,k'=1}^{15}c_k^{[4]}\xi_{k'}^{[4]}\int_0^{R_{\lim}}R^6$$
$$\times\exp[-(a_k^{[4]}+\kappa_{k'}^{[4]})R^2]dR. \qquad (82)$$

The functions $\chi_{00}(R)$ and $\chi_{nl}(p_0R)$ are determined by numerical solution of the Schrödinger equation with the potentials constructed in Ref. 22, using the elastic RGM and the experimental phase shifts.

In Fig. 24 we show the differential cross sections of the two-particle photodisintegration of the ^{4}He nucleus to the $d+d$ channel by photons of energies $E_\gamma=39.8$ and 45.3 MeV together with the experimental data of Ref. 108, calculated using Eq. (82), including only the $E2$ transition. In Fig. 25 we show these differential cross sections as functions of the energy $E_x=E_\gamma-Q$ ($Q=23.848$ MeV is the reaction threshold) at the angles $\vartheta=137°$ and $\vartheta=152°$ in the c.m. frame. We see that the agreement with the experimental data is not bad.

We note that there have also been earlier attempts to apply the potential description to the photonuclear reactions $d+d\to{}^3\text{He}\gamma$ and $^4\text{He}\gamma\to d+d$ (Refs. 74 and 76). For example, in Ref. 76 it was shown that the results of the potential description of the radiative capture reaction $d+d\to{}^4\text{He}\gamma$ depend strongly on small changes of the parameters of the interaction potential. On this basis it was concluded in that study and in Ref. 105 that the potential approach is altogether unsuitable for describing photonuclear reactions involving very light nuclei. From our point of view this conclusion is wrong. The reason is that the $d+d$ interaction potentials used in Ref. 76 are incorrect. In fact, as the interaction potential in the final channel with $[f]=[4]$ the authors of Ref. 76 chose a very shallow potential with depth of about 19 MeV. Obviously, this potential does not contain a bound state of the $d+d$ system—the ground state of the ^{4}He nucleus, so that it is not at all consistent with the potential determining the ground-state wave function of the ^{4}He nucleus. Only the use of the correct, microscopically justified interaction potentials [see (14)] leads to the correct description of photonuclear reactions involving two neutrons. This conclusion is also confirmed by the independent results of Ref. 74, where the two-neutron system in the final and initial states was described purely empirically using a Woods–Saxon interaction potential with the parameters

$$V_0=74.0\text{ MeV},\quad R_0=1.7\text{ F},\quad a=0.9\text{ F}.$$

It is easily verified that this potential is very close to the potential (14) and ensures an excellent description of the available experimental data on photonuclear reactions in a wide energy range.[74] Now we clearly see that the success here is due to the fact that the same Young scheme $[f]=[4]$ is realized in both the initial and the final state.

Now let us consider two-particle photodisintegration of the ^{4}He nucleus to the $p+{}^3\text{H}$ and $n+{}^3\text{He}$ channels. These mirror reactions are interesting because they may help to explain the possible violation of the charge independence of nuclear forces.[109] The reaction data are usually described using microscopic approaches like the

RGM. However, the same results can be obtained in the simple potential approach described in Secs. 1 and 2 for the systems $p+d$, $d+{}^3$He, and $d+d$.

From the ideological point of view the calculation of the differential cross section for α-particle two-particle photodisintegration is practically identical to the calculation of the cross section for the reaction ${}^3\mathrm{He}\gamma\to p+d$ studied earlier. As before, we include only $E1$, $E2$, and $M1$ transitions, which according to the results of Ref. 109 give the dominant contribution to the cross section for the reactions ${}^4\mathrm{He}\gamma\to p+{}^3\mathrm{H}$ and ${}^4\mathrm{He}\gamma\to n+{}^3\mathrm{He}$. We keep only the leading terms in the intercluster coordinate R in the operators for these transitions. As for the systems studied earlier, for the wave functions of the initial and final states we use the cluster wave functions of the ^{4}He nucleus as an $N+3N$ system in the continuum (the latter is either the $p+{}^3$H or the $n+{}^3$He system):

$$|i\rangle=\{\varphi(234)\chi_{00}(R)\,Y_{00}(\Omega_R)\}^{[4]}|[\tilde{4}]000\rangle, \tag{83}$$

$$|f\rangle\equiv\psi^{(-)}_{p_0}=\sqrt{2}\pi(-1)^{1/2\sigma'_A}\sum_{[f]}\left\{\sum_{lm} i^l\exp(-i\delta_l)\right.$$
$$\left.\times y^*_{lm}(\Omega_{p_0})\,Y_{lm}(\Omega_R)\chi_{nl}(p_0R)\varphi(234)\right\}^{[f]}\delta_{\sigma'_A,-\sigma'_B}|[\tilde{1}]$$
$$\times\frac{1}{2}\sigma'_A\frac{1}{2}\tau_A;[\tilde{3}]\,\frac{1}{2}\sigma'_B\frac{1}{2}\rho_B;[\tilde{4}]0000\rangle. \tag{84}$$

Here $\varphi(234)$ is the spatial part of the wave function of the bound three-nucleon subsystem (the ^{3}H or ^{3}He nucleus) consisting of the nucleons numbered 2, 3, 4; $\tau_A=1/2$, $\tau_B=-1/2$ for the $p+{}^3$He channel, and $\tau_A=-1/2$, $\tau_B=1/2$ for the $n+{}^3$He channel.

The wave functions (83) and (84) are antisymmetrized using the Young projection operators in the nonstandard basis corresponding to the reduction $U(4)\supset U(1)\times U(3)$ (see Ref. 23):

$$P^{[4]}_{[1][3];[1][3]}=\tfrac{1}{4}(E+P_{12}+P_{13}+P_{14}), \tag{85}$$

$$P^{[31]}_{[1][3];[1][3]}=\tfrac{1}{4}(3E-P_{12}-P_{13}-P_{14}). \tag{86}$$

The relative-motion functions $\chi_{00}(R)$ in (83) and $\chi_{nl}(p_0R)$ in (84) are found by numerically solving the Schrödinger equation with the interaction potentials $V^{[f]}_{L,t,S}$ constructed above. All the needed matrix elements can be obtained for these functions by using the Gaussian expansions (45) and (52). As an illustration, we write down the matrix element for the $E1$ electric dipole operator:

$$\langle f|\hat{T}^E_{|\lambda}|i^{[4]}\rangle$$
$$=(-1)^{1/2\sigma'_A}\delta_{\sigma'_A,-\sigma'_B}\frac{ik_\gamma e\sqrt{\pi}}{24\sqrt{2}}\exp(i\delta_1^{[31]})\,Y_{1\lambda}(\Omega_{p_0})$$
$$\times\sum_{k,k'=1}^{15}c_k^{[4]}\xi_{k'}^{[31]}\left\{\int_0^{R_{\lim}}R^4\right.$$
$$\times\exp\left(-(a_k^{[4]}+\kappa_{k'}^{[4]})R^2dR\right.$$
$$-\frac{16\pi^2}{3}\left[\frac{3\beta^4}{\pi^2}\right]^{3/2}\frac{4\Sigma_2+\Sigma_3}{\Sigma_3}\int_0^{R_{\lim}}R^4$$
$$\times\exp\left(-\frac{1}{2}\left(2\Sigma_1-\frac{\Sigma_2^2}{\Sigma_3}\right)R^2\right)dr\int_0^{R_{\lim}}x^2$$
$$\times\exp\left(-\frac{2}{9}\Sigma_3x^2\right)$$
$$\left.\left.\times dx\int_0^{R_{\lim}}r_{23}^2\exp\left(-\frac{3}{2}\beta^2r_{23}^2\right)dr_{23}\right\}, \tag{87}$$

where

$$\Sigma_1=\beta^2+a_k^{[4]}+\tfrac{1}{9}\kappa_{k'}^{[31]},\quad \Sigma_2=\beta^2-\tfrac{8}{9}\kappa_{k'}^{[31]},$$
$$\Sigma_3=5\beta^2+\frac{32}{9}\kappa_{k'}^{[31]},$$

and the value of $R_{\lim}$ is chosen on the basis of the stability condition for the values of the integrals in (87) [$R_{\lim}$ should not be greater than the length of the region in which the functions $\chi_{nl}(p_0R)$ and $\chi_{00}(R)$ are approximated by sums of Gaussians].

It is interesting to note that, as in the case of the $p+d$ system, the electric dipole transition is nondiagonal in the symmetry of the system, $[f]$. In addition,

$$\langle f|\hat{T}^M_{|\lambda}|i^{[4]}\rangle=0 \tag{88}$$

in complete analogy and for the same reasons as for the $p+d$ system.

The change of the normalization of the initial-state function (83) due to antisymmetrization is found by direct calculation:

$$(N^{[4]})^2=\frac{5}{8}N^2_{\text{before}}+6\pi^2\left[\frac{27\beta^4}{\pi^2}\right]^{3/2}\sum_{k,k'=1}^{15}c_k^{[4]}c_{k'}^{[4]}$$
$$\times\left\{\Sigma_4\left(16\Sigma_5\Sigma_6-\frac{\Sigma_7}{4}(4\Sigma_6+\Sigma_5+\Sigma_7)\right\}^{-3/2}, \tag{89}$$

where

$$\Sigma_4=\beta^2+a_k^{[4]}+\tfrac{1}{9}a_{k'}^{[4]},\quad \Sigma_5=\beta^2+\tfrac{4}{9}a_{k'}^{[4]},$$
$$\Sigma_6=\beta^2+\tfrac{1}{9}a_{k'}^{[4]},\quad \Sigma_7=\beta^2-\tfrac{8}{9}a_{k'}^{[4]}.$$

The procedure for calculating the changed normalization of the continuum function (84) is analogous to that described earlier for the $p+d$ system.

In Fig. 26 we show the differential cross section of the reaction ${}^4\mathrm{He}\gamma\to p+{}^3\mathrm{H}$ as a function of the proton emission angle θ (in the c.m. frame) together with the experimental data of Ref. 70 for two values of the γ energy, 27 and 29 MeV. In Fig. 27 we show the differential cross section of the reaction ${}^4\mathrm{He}\gamma\to n+{}^3\mathrm{He}$ for $E\gamma=29$ MeV. Here the experimental data are also taken from Ref. 70. We note that the dominant contribution to the cross section comes from the $E1$ transition. As can be seen from Figs. 26 and 27, the theoretically calculated cross sections are in good

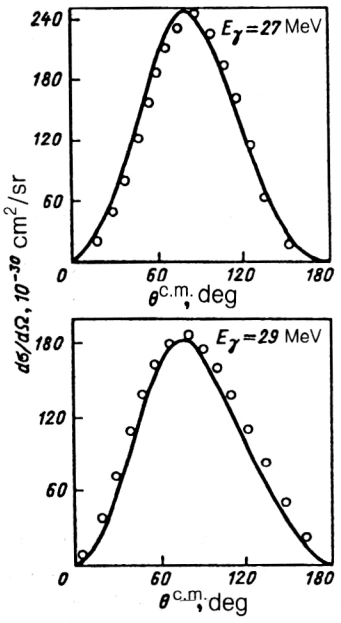

FIG. 26. Angular distributions for the reaction ^{4}He$\gamma\rightarrow p+^3$H at $E\gamma$=27 and 29 MeV. The experimental data are from Ref. 70.

agreement with the experimental data, and we therefore conclude that the potential approach is correct and promising.

CONCLUSION

We see that on the whole the optical model of nucleon scattering on nuclei proposed about forty years ago remains a viable and fruitful approach to the physically deep problem of composite-particle scattering, since it admits conceptual development and complexification. Using a very simple theoretical technique, we have predicted the cross sections with deuteron flip to the singlet state, which as yet are poorly studied experimentally. Here there is a broad area which deserves study. We have presented calculations of binary photonuclear reactions which show that the quantitative description of the experimental data in the region $E\gamma\leqslant 50$ MeV does not at all require complicated ground state wave functions of nuclei such as ^{3}He, ^{4}He, and ^{5}He (here the shell functions transformed to cluster channels are in fact sufficient), and that it is based on the correct inclusion of the final-state interaction, where amplitudes with different symmetry $[f]$ can interfere. The pairs of nuclei that we have studied are important for the physics of fusion reactions. The theoretical scheme outlined here is easily generalized, for example, to ^{6}Li+d, ^{6}Li+h, ^{6}Li+^{6}Li, etc., scattering. It is also applicable for treating spin–isospin flip $N+N\rightarrow\Delta+\Delta$ and, more generally, $N+N\rightarrow N^*+N^*$ at energies of several GeV, since the quark description of nucleons in the NN system is at present constructed in many studies by using also the quantum numbers of the permutation symmetry $[f]$; the difference is that the unitary symmetry groups used here are more complicated than $SU(4)$.

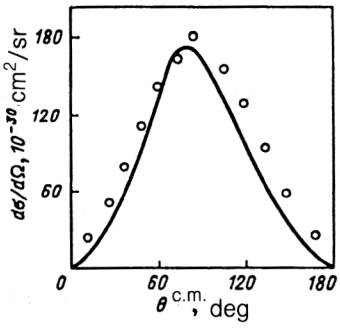

FIG. 27. Angular distribution for the reaction ^{4}He$\gamma\rightarrow n+^3$He at $E\gamma$=29 MeV. The experimental data are from Ref. 70.

APPENDIX

Here we give a detailed derivation of the matrix element for the operator of the $E1$ transition from the ground state of the ^{3}He nucleus to the continuum of the $p+d$ system.

According to (42), the wave function of the initial state (the $J^\pi=\frac{1}{2}^+$ ground state of the ^{3}He nucleus) in the cluster representation is written as

$$|i^{[3]}\rangle=\frac{1}{6\sqrt{\pi}}\{\varphi(23)\chi_{00}(R)+\varphi(13)\chi_{00}(R')+\varphi(21)\chi_{00}(R'')\}|[\tilde{3}]^{\frac{1}{2}}\sigma\tfrac{1}{2}\tfrac{1}{2}\rangle. \quad (A1)$$

The wave function of the final state (the continuum of the $p+d$ system) is

$$|f^{[f]}\rangle=\sum_{s,\sigma,[f]}\left\{4\pi\sum_{lm}i^l\exp(-i\delta_l)\,Y^*_{lm}(\Omega_{p_0})\times Y_{lm}(\Omega_R)\chi_{nl}(p_0R)\varphi(23)\right\}^{[f]}\times\langle[\tilde{1}]^{11}_{22},[\tilde{2}]10|[\tilde{f}]S^1_2\rangle(\tfrac{1}{2}\sigma'_A,l\sigma'_B|S\sigma)|[\tilde{1}]\times\tfrac{1}{2}\sigma'_A\tfrac{1}{2}\tfrac{1}{2};[\tilde{2}]1\sigma'_B00:[\tilde{f}]S\sigma\tfrac{1}{2}\tfrac{1}{2}\rangle. \quad (A2)$$

Since the electric dipole operator $\hat{T}^{E1}_{1\lambda}$ (39) does not contain any spin dependence, the spins of the initial and final states coincide, $S=\frac{1}{2}$. Among all the possible values of the isoscalar factors of the Clebsch–Gordan coefficients of the group $SU(4)$, $\langle[\tilde{1}]^{11}_{22},[\tilde{2}]10|[\tilde{f}]^{11}_{22}\rangle$, only two are nonzero: one corresponds to the symmetry $[\tilde{f}]=[\tilde{2}1]$ and the other to $[\tilde{f}]=[\tilde{3}]$. Therefore, the matrix element for the $E1$ operator (transition to the P wave) becomes

$$\langle f|\hat{T}^{E1}_{1\lambda}|i^{[3]}\rangle=-\frac{2\pi}{\sqrt{3}}i\left(\frac{1}{2}\sigma'_A,1\sigma'_B|\frac{1}{2}\sigma\right)\times\left\{\sum_{j=1}^{9}\mathscr{U}_j+\sum_{j=1}^{}\mathscr{B}_j\right\}, \quad (A3)$$

where the symbols $\mathscr{U}_j$ denote the parts of the matrix element corresponding to the transition nondiagonal in the symmetry $[f]$ (from $[f]=[3]$ to $[f]=[21]$), and the sym-

bols $\mathscr{B}_j$ denote the parts corresponding to the diagonal transition (from $[f]=[3]$ to $[f]=[3]$). For what follows it is convenient to have the explicit expressions for $\mathscr{U}_j$:

$$\mathscr{U}_1=\frac{2}{3}i\exp(i\delta_1^{[21]})\sum_m Y_{1m}(\Omega_{p_0})\int Y_{1m}^*(\Omega_R)\chi_{n1}^{[21]} \times(p_0R)\varphi(23)\hat{T}_{1\lambda}^{E1}\chi_{00}^{[3]}(R)\varphi(23)d\mathbf{r}_{23}d\mathbf{R}, \quad \text{(A4)}$$

$$\mathscr{U}_2=\frac{1}{3}i\exp(i\delta_1^{[21]})\sum_m Y_{im}(\Omega_{p_0})\int Y_{1m}^*(\Omega_{R'})\chi_{n1}^{[21]} \times(p_0R')\varphi(13)\hat{T}_{1\lambda}^{E1}\chi_{00}^{[3]}(R)\varphi(23)d\mathbf{r}_{23}d\mathbf{R}, \quad \text{(A5)}$$

$$\mathscr{U}_3=\frac{1}{3}i\exp(i\delta_1^{[21]})\sum_m Y_{1m}(\Omega_{p_0})\int Y_{1m}^*(\Omega_{R''})\chi_{n1}^{[21]} \times(p_0R''))\varphi(21)\hat{T}_{1\lambda}^{E1}\chi_{00}^{[3]}(R)\varphi(23)d\mathbf{r}_{23}d\mathbf{R}, \quad \text{(A6)}$$

$$\mathscr{U}_4=-\frac{2}{3}i\exp(i\delta_1^{[21]})\sum_m Y_{1m}(\Omega_{p_0})\int Y_{1m}^*(\Omega_R)\chi_{n1}^{[21]} \times(p_0R)\varphi(23)\hat{T}_{1\lambda}^{E1}\chi_{00}^{[3]}(R')\varphi(13)d\mathbf{r}_{23}d\mathbf{R}, \quad \text{(A7)}$$

$$\mathscr{U}_5=\frac{1}{3}i\exp(i\delta_1^{[21]})\sum_m Y_{1m}(\Omega_{p_0})\int Y_{1m}^*(\Omega_{R'})\chi_{n1}^{[21]} \times(p_0R')\varphi(13)\hat{T}_{1\lambda}^{E1}\chi_{00}^{[3]}(R')\varphi(13)d\mathbf{r}_{23}d\mathbf{R}, \quad \text{(A8)}$$

$$\mathscr{U}_6=\frac{1}{3}i\exp(i\delta_1^{[21]})\sum_m Y_{1m}(\Omega_{p_0})\int Y_{1m}^*(\Omega_{R''})\chi_{n1}^{[21]} \times(p_0R'')\varphi(21)\hat{T}_{1\lambda}^{E1}\chi_{00}^{[3]}(R')\varphi(13)d\mathbf{r}_{23}d\mathbf{R}, \quad \text{(A9)}$$

$$\mathscr{U}_7=-\frac{2}{3}i\exp(i\delta_1^{[21]})\sum_m Y_{1m}(\Omega_{p_0})\int Y_{1m}^*(\Omega_R)\chi_{n1}^{[21]} \times(p_0R)\varphi(23)\hat{T}_{1\lambda}^{E1}\chi_{00}^{[3]}(R'')\varphi(21)d\mathbf{r}_{23}d\mathbf{R}, \quad \text{(A10)}$$

$$\mathscr{U}_8=\frac{1}{3}i\exp(i\delta_1^{[21]})\sum_m Y_{1m}(\Omega_{p_0})\int Y_{1m}^*(\Omega_{R'})\chi_{n1}^{[21]} \times(p_0R')\varphi(13)\hat{T}_{1\lambda}^{E1}\chi_{00}^{[3]}(R'')\varphi(21)d\mathbf{r}_{23}d\mathbf{R}, \quad \text{(A11)}$$

$$\mathscr{U}_9=\frac{1}{3}i\exp(i\delta_1^{[21]})\sum_m Y_{1m}(\Omega_{p_0})\int Y_{1m}^*(\Omega_{R''})\chi_{n1}^{[21]} \times(p_0R'')\varphi(21)\hat{T}_{1\lambda}^{E1}\chi_{00}^{[3]}(R'')\varphi(21)d\mathbf{r}_{23}d\mathbf{R}. \quad \text{(A12)}$$

The expressions for $\mathscr{B}_j$ are analogous Eqs. (A4)–(A12) above; only the phase shifts $\delta_L^{[f]}$ are changed to correspond to the relative-motion functions $\chi_{n1}^{[f]}(p_0R)$: in the case of $\mathscr{U}_j$ they correspond to the symmetry $[f]=[21]$, and in the case of $\mathscr{B}_j$ they correspond to $[f]=[3]$. Formally, we can write (up to the substitutions mentioned above)

$$\mathscr{B}_1=\tfrac{1}{2}\mathscr{U}_1,\quad \mathscr{B}_2=-\mathscr{U}_2,\quad \mathscr{B}_3=-\mathscr{U}_3,\quad \mathscr{B}_4=\tfrac{1}{2}\mathscr{U}_4,$$

$$\mathscr{B}_5=-\mathscr{U}_5,\quad \mathscr{B}_6=-\mathscr{U}_6,\quad \mathscr{B}_7=\tfrac{1}{2}\mathscr{U}_7,$$

$$\mathscr{B}_8=-\mathscr{U}_8,\quad \mathscr{B}_9=-\mathscr{U}_9. \quad \text{(A13)}$$

In Eqs. (A4)–(A6) the $E1$ operator acts on the cluster wave function of the system

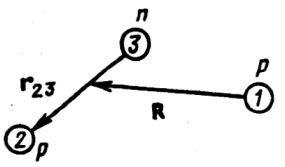

This operator, written in the form (39), is a function of the single-particle coordinates $\mathbf{r}_j$, while the initial- and final-state wave functions in the matrix element (A3) are functions of the Jacobi coordinates. Therefore, also in the operator $\hat{T}_{1\lambda}^{E1}$ we need to transform to the Jacobi coordinates $\mathbf{r}_{23}$ and $\mathbf{R}$. In these coordinates $\hat{T}_{1\lambda}^{E1}$ is rewritten as

$$\hat{T}_{1\lambda}^{E1}=-\frac{\sqrt{2}}{3}k_\gamma e\left\{\frac{1}{2}r_{23}Y_{1\lambda}(\Omega_{r_{23}})-\frac{1}{3}RY_{1\lambda}(\Omega_R)\right\}. \quad \text{(A14)}$$

Using (A14), we can easily calculate the values of (A4)–(A6) for $\mathscr{U}_1$, $\mathscr{U}_2$, and $\mathscr{U}_3$. In fact,

$$\mathscr{U}_1=\frac{2\sqrt{2}}{9}iek_\gamma\exp(i\delta_1^{[21]})\sum_m Y_{1m}(\Omega_{p_0}) \times\left\{\frac{1}{2}\int Y_{1m}^*(\Omega_R)\chi_{n1}^{[21]}(p_0R) \times\varphi(23)r_{23}Y_{1\lambda}(\Omega_{r_{23}}) \times\chi_{00}^{[3]}(R)\varphi(23)d\mathbf{r}_{23}d\mathbf{R}-\frac{1}{3}\int Y_{1m}^*(\Omega_R)\chi_{n1}^{[21]} \times(p_0R)\varphi(23)RY_{1\lambda}(\Omega_R)\chi_{00}^{[3]}(R)\varphi(23)d\mathbf{r}_{23}d\mathbf{R}\right\}. \quad \text{(A15)}$$

Since

$$\int Y_{1\lambda}(\Omega_{r_{23}})d\Omega_{r_{23}}=\delta_{0,1}\delta_{\lambda,0}=0,$$

only the second term remains in (A15). Using the expansions (45) and (52), we obtain

$$\mathscr{U}_1=-\frac{2\sqrt{2}}{27}iek_\gamma\exp(i\delta_1^{[21]})Y_{1\lambda}(\Omega_{p_0})\sum_{k,k'}c_k^{[3]}\xi_{k'}^{[21]} \times\int_0^{R_{\lim}}R^4\exp[-(a_k^{[3]}+\kappa_{k'}^{[21]})R^2]d\mathbf{R}. \quad \text{(A16)}$$

In the case of $\mathscr{U}_2$ the situation is somewhat more complicated. Here

$$\mathcal{U}_2=-\frac{\sqrt{2}}{9}iek_\gamma\exp(i\delta_1^{[21]})\sum_m Y_{1m}(\Omega_{p_0})$$
$$\times\left\{\frac{1}{2}\int Y_{1m}^*(\Omega_{R'})\chi_{n1}^{[21]}(p_0R')\varphi(13)r_{23}Y_{1\lambda}(\Omega_{r_{23}})\right.$$
$$\times\chi_{00}^{[3]}(R)\varphi(23)d\mathbf{r}_{23}d\mathbf{R}-\frac{1}{3}\int Y_{1m}^*(\Omega_{R'}\chi_{n1}^{[21]}$$
$$\left.\times(p_0R')\varphi(13)RY_{1\lambda}(\Omega_R)\chi_{00}^{[3]}(R)\varphi(23)d\mathbf{r}_{23}d\mathbf{R}\right\}$$
$$=-\frac{\sqrt{2}}{9}iek_\gamma\exp(i\delta_1^{[21]})\sum_m Y_{1m}(\Omega_{p_0})[\mathcal{U}_2^M+\mathcal{U}_2^0], \tag{A17}$$

$$\mathcal{U}_2^M=-\frac{1}{3}\left[\frac{\alpha}{\pi}\right]^{3/2}\sum_{k,k'}c_k^{[3]}\xi_{k'}^{[21]}\int R'Y_{1m}^*(\Omega_{R'})RY_{1\lambda}(\Omega_R)$$
$$\times\exp\left(-\frac{1}{2}\alpha r_{13}^2-\frac{1}{2}\alpha r_{23}^2-a_k^{[3]}R^2\right.$$
$$\left.-\kappa_{k'}^{[21]}R'^2\right)d\mathbf{r}_{23}d\mathbf{R}. \tag{A18}$$

We isolate the total square in the exponent of (A18), using the relation between different sets of Jacobi coordinates (55):

$$-\frac{1}{2}\alpha r_{13}^2-\frac{1}{2}\alpha r_{23}^2-a_k^{[3]}R^2-\kappa_{k'}^{[21]}R'^2$$
$$=-\frac{1}{16}(10\alpha+9\kappa_{k'}^{[21]})\left(\mathbf{r}_{23}-2\frac{2\alpha-3\kappa_{k'}^{[21]}}{10\alpha+9\kappa_{k'}^{[21]}}\mathbf{R}\right)^2$$
$$-\frac{1}{4}\left(2\alpha+4a_k^{[3]}+\kappa_{k'}^{[21]}-\frac{(2\alpha-3\kappa_{k'}^{[21]})^2}{10\alpha+9\kappa_{k'}^{[21]}}\right)R^2, \tag{A19}$$

and then transform from the old coordinates $\mathbf{r}_{23}$, $\mathbf{R}$ to the new ones

$$\mathbf{y}=\mathbf{r}_{23}-2\frac{2\alpha-3\kappa_{k'}^{[21]}}{10\alpha+9\kappa_{k'}^{[21]}}\mathbf{R},\mathbf{R}.$$

The Jacobian of this transformation is unity. We also take into account the fact that

$$R'Y_{1m}^*(\Omega_{R'})=\mathcal{Y}_{1m}^*(R')=\mathcal{Y}_{1m}^*(-\tfrac{3}{4}\mathbf{r}_{23}-\tfrac{1}{2}\mathbf{R})$$
$$=-\tfrac{3}{4}r_{23}Y_{1m}^*(\Omega_{r_{23}})-\tfrac{1}{2}RY_{1m}^*(\Omega_R), \tag{A20}$$

and, therefore,

$$\mathcal{U}_2^M=-\frac{1}{3}\left[\frac{\alpha}{\pi}\right]^{3/2}\sum_{k,k'}c_k^{[3]}\xi_{k'}^{[21]}\left\{-\frac{3}{4}\mathcal{U}_{21}^M-\frac{1}{2}\mathcal{U}_{22}^M\right\}, \tag{A21}$$

where

$$\mathcal{U}_{21}^M=\int r_{23}Y_{1m}^*(\Omega_{r_{23}})RY_{1\lambda}(\Omega_R)\exp\left(-\frac{1}{16}(10\alpha\right.$$
$$\left.+9\kappa_{k'}^{[21]})y^2\right)\exp\left(-\frac{1}{4}\left(2\alpha+4a_k^{[3]}+\kappa_{k'}^{[21]}\right.\right.$$
$$\left.\left.-\frac{(2\alpha-3\kappa_{k'}^{[21]})^2}{10\alpha+9\kappa_{k'}^{[21]}}\right)R^2\right)d\mathbf{r}_{23}d\mathbf{R}, \tag{A22}$$

$$\mathcal{U}_{22}^M=4\pi\delta_{m,\lambda}\int_0^{R_{\lim}}y^2\exp\left(-\frac{1}{16}(10\alpha\right.$$
$$\left.+9\kappa_{k'}^{[21]})y^2\right)dy\int_0^{R_{\lim}}R^4\exp\left(-\frac{1}{4}\left(2\alpha+4a_k^{[3]}\right.\right.$$
$$\left.\left.+\kappa_{k'}^{[21]}-\frac{(2\alpha-3\kappa_{k'}^{[21]})^2}{10\alpha+9\kappa_{k'}^{[21]}}\right)R^2\right)dR. \tag{A23}$$

Equation (A22) also is easily reduced to trivial integrals of the type (A23) after a transformation analogous to (A20):

$$r_{23}Y_{1m}^*(\Omega_{r_{23}})=\mathcal{Y}_{1m}^*(\mathbf{r}_{23})=\mathcal{Y}_{1m}^*\left(y+2\frac{2\alpha-3\kappa_{k'}^{[21]}}{10\alpha+9\kappa_{k'}^{[21]}}\mathbf{R}\right)$$
$$=yY_{1m}^*(\Omega_y)+2\frac{2\alpha-3\kappa_{k'}^{[21]}}{10\alpha+9\kappa_{k'}^{[21]}}\mathbf{R}Y_{1m}^*(\Omega_{R'}).$$

Then

$$\mathcal{U}_{21}^M=8\frac{2\alpha-3\kappa_{k'}^{[21]}}{10\alpha+9\kappa_{k'}^{[21]}}\pi\delta_{m,\lambda}\int_0^{R_{\lim}}y^2\exp\left(-\frac{1}{16}(10\alpha\right.$$
$$\left.+9\kappa_{k'}^{[21]})y^2\right)dy\int_0^{R_{\lim}}R^4\exp\left(-\frac{1}{4}\left(2\alpha\right.\right.$$
$$\left.\left.+4a_k^{[3]}+\kappa_{k'}^{[21]}-\frac{(2\alpha-3\kappa_{k'}^{[21]})^2}{10\alpha+9\kappa_{k'}^{[21]}}\right)R^2\right)d\mathbf{R}. \tag{A24}$$

We calculate $\mathcal{U}_2^0$ in a similar manner:

$$\mathcal{U}^0=-\frac{1}{3}\left[\frac{\alpha}{\pi}\right]^{3/2}\sum_{k,k'}c_k^{[3]}\xi_{k'}^{[21]}\left\{-\frac{3}{4}\mathcal{U}_{21}^0-\frac{1}{2}\mathcal{U}_{22}^0\right\}, \tag{A25}$$

$$\mathcal{U}_{21}^{0}=4\pi\delta_{m,\lambda}\int_0^{R_{\lim}} r_{23}^4 \exp\left(-\frac{1}{16}\left(10\alpha+9\kappa_{k'}^{[21]}-\frac{(2\alpha-3\kappa_{k'}^{[21]})^2}{2\alpha+4a_k^{[3]}+\kappa_{k'}^{[21]}}\right)r_{23}^2\right)dr_{23}\int_0^{R_{\lim}} y^2 \times\exp\left[-\frac{1}{4}(2\alpha+4a_k^{[3]}+\kappa_{k'}^{[21]})y^2\right]dy, \quad \text{(A26)}$$

$$\mathcal{U}_{22}^{0}=2\frac{2\alpha-3\kappa_{k'}^{[21]}}{2\alpha+4a_k^{[3]}+\kappa_{k'}^{[21]}}\pi\delta_{m,\lambda}\int_0^{R_{\lim}} y^2 \times\exp\left[-\frac{1}{4}(2\alpha+4a_k^{[3]}+\kappa_{k'}^{[21]})y^2\right] \times dy\int_0^{R_{\lim}} r_{23}^4\times\exp\left(-\frac{1}{16}\left(10\alpha+9\kappa_{k'}^{[21]}-\frac{(2\alpha-3\kappa_{k'}^{[21]})^2}{2\alpha+4a_k^{[3]}+\kappa_{k'}^{[21]}}\right)r_{23}^2\right)dr_{23}. \quad \text{(A27)}$$

Now we turn to the calculation of Eq. (A6) for $\mathcal{U}_3$. Here

$$\mathcal{U}_3=-\frac{\sqrt{2}}{9}iek_\gamma\exp(i\delta_1^{[21]})\sum_m Y_{1m}(\Omega_{p_0}) \times\left\{\frac{1}{2}\int Y_{1m}^*(\Omega_{R''})\chi_{n1}^{[21]} \times(p_0R'')\varphi(21)r_{23}Y_{1\lambda}(\Omega_{r_{23}}) \times\chi_{00}^{[3]}(R)\varphi(23)d\mathbf{r}_{23}d\mathbf{R}-\frac{1}{3}\int Y_{1m}^*(\Omega_{R''})\chi_{n1}^{[21]} \times(p_0R'')\varphi(21)RY_{1\lambda}(\Omega_R)\chi_{00}^{[3]}(R)\varphi(23)d\mathbf{r}_{23}d\mathbf{R}\right\} =-\frac{\sqrt{2}}{9}iek_\gamma\exp(i\delta_1^{[21]})\sum_m Y_{1m}(\Omega_{p_0})[\mathcal{U}_3^M+\mathcal{U}_3^0], \quad \text{(A28)}$$

$$\mathcal{U}_3^M=-\frac{1}{3}\left[\frac{\alpha}{\pi}\right]^{3/2}\sum_{k,k'}c_k^{[3]}\xi_{k'}^{[21]}\int R''^*_{1m}(\Omega_{R''})RY_{1\lambda}(\Omega_R) \times\exp\left(-\frac{1}{2}gar_{21}^2-\frac{1}{2}\alpha r_{23}^2-a_k^{[3]}R^2-\kappa_{k'}^{[21]}R''^2\right) \times d\mathbf{r}_{23}d\mathbf{R}. \quad \text{(A29)}$$

Isolating the total square in the exponent of (A29)

$$-\frac{1}{2}\alpha r_{21}^2-\frac{1}{2}\alpha r_{23}^2-a_k^{[3]}R^2-\kappa_{k'}^{[21]}R''^2 =-\frac{1}{16}(10\alpha+9\kappa_{k'}^{[21]})\left(\mathbf{r}_{23}+2\frac{2\alpha-3\kappa_{k'}}{10\alpha+9\kappa_{k'}^{[21]}}\mathbf{R}\right)^2 -\frac{1}{4}\left(2\alpha+4a_k^{[3]}+\kappa_{k'}^{[21]}-\frac{(2\alpha-3\kappa_{k'})^2}{10\alpha+9\kappa_{k'}^{[21]}}\right)R^2,$$

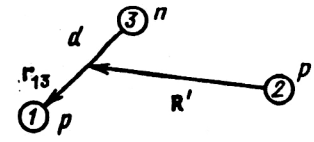

EQ (P) [between (A35)&(A36)]: 5 pica Depth

and using the relation

$$R''Y_{1m}^*(\Omega_{R''})=\mathcal{Y}_{1m}^*(R'')=\mathcal{Y}_{1m}^*(\tfrac{3}{4}\mathbf{r}_{23}-\tfrac{1}{2}\mathbf{R}) =\tfrac{3}{4}r_{23}Y_{1m}^*(\Omega_{r_{23}})-\tfrac{1}{2}RY_{1m}^*(\Omega_R),$$

we find that

$$\mathcal{U}_3^M=\mathcal{U}_2^M. \quad \text{(A30)}$$

Similarly,

$$\mathcal{U}_3^0=\mathcal{U}_2^0. \quad \text{(A31)}$$

In calculating $\mathcal{U}_4-\mathcal{U}_6$ it is necessary to take into account the fact that the $E1$-transition operator acts in the "rearranged" system, which now has the form

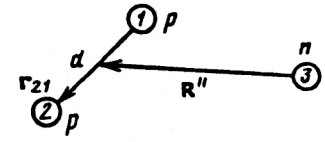

Transforming to the set of Jacobi coordinates in (39), we obtain

$$\hat{T}_{1\lambda}^{E1}=-\frac{\sqrt{2}}{3}k_\gamma e\left\{\frac{1}{2}r_{13}Y_{1\lambda}(\Omega_{r_{13}})-\frac{1}{3}R'Y_{1\lambda}(\Omega_{R'})\right\}. \quad \text{(A32)}$$

The rest of the calculations are completely analogous to those carried out above, and therefore we give only the final expressions for $\mathcal{U}_4-\mathcal{U}_6$:

$$\mathcal{U}_4=\frac{2\sqrt{2}}{9}iek_\gamma\exp(i\delta_1^{[21]})Y_{1\lambda}(\Omega_{p_0})[\mathcal{U}_2^M+\mathcal{U}_2^0], \quad \text{(A33)}$$

$$\mathcal{U}_5=-\tfrac{1}{2}\mathcal{U}_1, \quad \text{(A34)}$$

$$\mathcal{U}_6=-\frac{\sqrt{2}}{9}iek_\gamma\exp(i\delta_1^{[21]})Y_{1\lambda}(\Omega_{p_0})[\mathcal{U}_2^M-\mathcal{U}_2^0]. \quad \text{(A35)}$$

Calculating the values of $\mathcal{U}_7-\mathcal{U}_9$, we again rearrange the $E1$ transition operator. Now it acts in a different system and has a different form:

$$\hat{T}_{1\lambda}^{E1}=-\frac{2\sqrt{2}}{9}ek_\gamma R''Y_{1\lambda}(\Omega_{R''}). \quad \text{(A36)}$$

Then after trivial calculations we obtain

$$\mathcal{U}_7=-\frac{4\sqrt{2}}{9}iek_\gamma\exp(i\delta_1^{[21]})Y_{1\lambda}(\Omega_{p_0})\mathcal{U}_2^M, \qquad (A37)$$

$$\mathcal{U}_8=\frac{2\sqrt{2}}{9}iek_\gamma\exp(i\delta_1^{[21]})Y_{1\lambda}(\Omega_{p_0})\mathcal{U}_2^M, \qquad (A38)$$

$$\mathcal{U}_9=\mathcal{U}_1. \qquad (A39)$$

Collecting Eqs. (A16), (A17), (A23), (A28)–(A30), (A31), (A33)–(A35), and (A37)–(A39), we have

$$\sum_{j=1}^{9}\mathcal{U}_j=-\frac{\sqrt{2}}{9}iek_\gamma\exp(i\delta_1^{[21]})Y_{1\lambda}(\Omega_{p_0})\sum_{k,k'}c_k^{[3]}\xi_{k'}^{[21]}\left\{\int_0^{R_{\lim}}R^4\exp[-(a_k^{[3]}+\kappa_{k'}^{[21]})R^2]dR+\frac{2}{\sqrt{\pi}}\alpha^{3/2}\left[3\frac{2\alpha-3\kappa_{k'}^{[21]}}{10\alpha+9\kappa_{k'}^{[21]}}+1\right]\right.$$
$$\times\int_0^{R_{\lim}}R^4\exp\left[-\frac{1}{4}\left(2\alpha+4a_k^{[3]}+\kappa_{k'}^{[21]}-\frac{(2\alpha-3\kappa_{k'}^{[21]})^2}{10\alpha+9\kappa_{k'}^{[21]}}\right)R^2\right]dR$$
$$\times\int_0^{R_{\lim}}y^2\exp\left[-\frac{1}{16}(10\alpha+9\kappa_{k'}^{[21]})y^2\right]dy+\frac{3}{2\sqrt{\pi}}\alpha^{3/2}\left[3\frac{2\alpha-3\kappa_{k'}^{[21]}}{10\alpha+9\kappa_{k'}^{[21]}}+3\right]$$
$$\times\int_0^{R_{\lim}}r_{23}^4\exp\left[-\frac{1}{16}\left(10\alpha+9\kappa_{k'}^{[21]}-\frac{(2\alpha-3\kappa_{k'}^{[21]})^2}{2\alpha+4a_k^{[21]}+\kappa_{k'}^{[21]}}\right)r_{23}^2\right]$$
$$\left.\times dr_{23}\int_0^{R_{\lim}}y^2\exp\left[-\frac{1}{4}(2\alpha+4a_k^{[3]}+\kappa_{k'}^{[21]})y^2\right]dy\right\}. \qquad (A40)$$

For transitions occurring with conservation of the symmetry of the system, $[f]$, taking into account (A13), we formally obtain

$$\sum_{j=1}^{9}\mathcal{B}_j=\frac{1}{2}\mathcal{U}_1-\mathcal{U}_2-\mathcal{U}_3+\frac{1}{2}\mathcal{U}_4-\mathcal{U}_5-\mathcal{U}_6+\frac{1}{2}\mathcal{U}_7$$
$$-\mathcal{U}_8-\mathcal{U}_9$$
$$=\left(\frac{1}{2}\mathcal{U}_1-\mathcal{U}_5-\mathcal{U}_9\right)-\left(\mathcal{U}_2+\mathcal{U}_3-\frac{1}{2}\mathcal{U}_4+\mathcal{U}_6\right.$$
$$\left.-\frac{1}{2}\mathcal{U}_7+\mathcal{U}_8\right)$$
$$=\left(\frac{1}{2}\mathcal{U}_1+\frac{1}{2}\mathcal{U}_1-\mathcal{U}_1\right)-\text{const}\left[\frac{\sqrt{2}}{9}(\mathcal{U}_2^0+\mathcal{U}_2^M)\right.$$
$$+\frac{\sqrt{2}}{9}(\mathcal{U}_2^M-\mathcal{U}_2^0)+\frac{\sqrt{2}}{9}(\mathcal{U}_2^0+\mathcal{U}_2^M)+\frac{\sqrt{2}}{9}(\mathcal{U}_2^M$$
$$\left.-\mathcal{U}_2^0)-\frac{2\sqrt{2}}{9}\mathcal{U}_2^M-\frac{2\sqrt{2}}{9}\mathcal{U}_2^M\right]=0. \qquad (A41)$$

[1] V. G. Neudatchin, V. I. Kukulin, V. P. Korennoy, and V. L. Korotkih, Phys. Lett. **34B**, 581 (1971).
[2] V. G. Neudatchin, A. N. Boyarkina, V. P. Korennoy, and V. I. Kukulin, Lett. Nuovo Cimento **5**, 834 (1972).
[3] I. V. Kurdumov, V. G. Neudatchin, Yu. F. Smirnov, V. P. Korennoy, Phys. Lett. **40B**, 607 (1972).
[4] V. I. Kukulin, V. G. Neudatchin, and Yu. F. Smirnov, Nucl. Phys. **A245**, 429 (1975).
[5] S. Saito, Prog. Theor. Phys. **41**, 705 (1969).
[6] K. Wildermuth and Y. C. Tang, *A Unified Theory of the Nucleus* (Academic Press, New York, 1977) [Russian transl., Mir, Moscow, 1980].
[7] P. Swan, Proc. R. Soc. London A **228**, 10 (1955); Ann. Phys. (N.Y.) **48**, 455 (1968).
[8] K. Aoki and H. Horiuchi, Prog. Theor. Phys. **69**, 516, 857 (1983).
[9] J. C. Fong, M. M. Gazzaly, G. Igo *et al.*, Nucl. Phys. **A262**, 365 (1976).
[10] R. A. Baldock, B. A. Robson, and R. F. Barrett, Nucl. Phys. **A366**, 270 (1981); **A381**, 138 (1982); K. Naiddo, H. Fiedeldey, S. A. Sofianos, and R. Lipperheide, Nucl. Phys. **A419**, 23 (1984).
[11] W. Von Oertzen and H. G. Bohlen, Phys. Rev. C **19**, 1 (1979); W. Von Oertzen and B. Imanishi, Nucl. Phys. **A424**, 262 (1984).
[12] Dao Tien Khoa and K. V. Shitikova, Yad. Fiz. **41**, 1166 (1985) [Sov. J. Nucl. Phys. **41**, 745 (1985)].
[13] V. G. Neudachin and Yu. F. Smirnov, in *Current Problems in Optics and Nuclear Physics* [in Russian], edited by G. F. Filippov (Naukova Dumka, Kiev, 1974), p. 225.
[14] Yu. F. Smirnov, I. T. Obukhovsky, Yu. M. Tchuvilsky, and V. G. Neudatchin, Nucl. Phys. **A235**, 289 (1974).
[15] A. C. Fonseca, J. Revai, and A. Matveenko, Nucl. Phys. **A326**, 182 (1979); **A342**, 444 (1980).
[16] N. A. Burkova and M. A. Zhusupov, Izv. Akad. Nauk SSSR, Ser. Fiz. **51**, 182 (1987) [Bull. Acad. Sci. USSR, Phys. Ser.].
[17] Yu. L. Dorodnykh, V. G. Neudachin, and N. P. Yudin, Yad. Fiz. **48**, 1796 (1988) [Sov. J. Nucl. Phys. **48**, 1081 (1988)].
[18] V. Iskra, A. I. Mazur, V. G. Neudachin, and Yu. F. Smirnov, Yad. Fiz. **48**, 1674 (1988) [Sov. J. Nucl. Phys. **48**, 1003 (1988)].
[19] S. B. Dubovichenko, V. G. Neudachin, A. A. Sakharuk, and Yu. F. Smirnov, Izv. Akad. Nauk SSSR, Ser. Fiz. **54**, 911 (1990) [Bull. Acad. Sci. USSR, Phys. Ser.].
[20] V. I. Kukulin, V. G. Neudachin, V. N. Pomerantsev, and A. A. Sakharuk, Yad. Fiz. **52**, 402 (1990) [Sov. J. Nucl. Phys. **52**, 258 (1990)].
[21] L. Tomio and S. K. Adhikari, Phys. Rev. C **35**, 441 (1987).
[22] N. M. Petrov, Yad. Fiz. **48**, 50 (1988) [Sov. J. Nucl. Phys. **48**, 31 (1988)].
[23] D. R. Tilley, H. R. Weller, and H. H. Hasan, Nucl. Phys. **A474**, 1 (1987).
[24] C. Werntz, Phys. Rev. C **27**, 1375 (1983); **24**, 349 (1981).
[25] F. Ajzenberg-Selove, Nucl. Phys. **A413**, 1 (1984).
[26] V. I. Kukulin, V. G. Neudachin, and Yu. F. Smirnov, Fiz. Elem. Chastits At. Yadra **10**, 1236 (1979) [Sov. J. Part. Nucl. **10**, 492 (1979)].

[27] V. I. Kukulin, V. G. Neudatchin, I. T. Obukhovsky, and Yu. F. Smirnov, in *Clustering Phenomena in Nuclei*, Vol. 3, edited by K. Wildermuth and P. Kramer (Vieweg, Wiesbaden, 1983), p. 1.
[28] M. Hamermesh, *Group Theory and Its Applications to Physical Problems* (Addison-Wesley, Reading, Mass., 1962) [Russian transl., Mir, Moscow, 1966].
[29] O. F. Nemets, V. G. Neudachin, A. T. Rudchik *et al.*, in *Nucleon Associations in Nuclei and Multinucleon Transfer Reactions* [in Russian] (Naukova Dumka, Kiev, 1988).
[30] H. Friedrich, Phys. Rep. **41**, 209 (1981).
[31] G. John and T. H. Seligman, Nucl. Phys. **A236**, 397 (1974).
[32] H. H. Hackenbroich and T. H. Seligman, Phys. Lett. **41B**, 102 (1972).
[33] J. Niewisch and D. Fick, Nucl. Phys. **A252**, 109 (1975).
[34] G. John and P. Kramer, Nucl. Phys. **A204**, 203 (1973).
[35] Lien Pham Dien, Nucl. Phys. **A178**, 375 (1972).
[36] H. Kanada, T. Kaneko, and Y. C. Tang, Phys. Rev. C **34**, 22 (1986).
[37] V. G. Neudachin and Yu. F. Smirnov, *Nucleon Associations in Light Nuclei* [in Russian] (Nauka, Moscow, 1969).
[38] M. A. Lane, Nucl. Phys. **A35**, 676 (1962).
[39] S. Fiarman and W. E. Meyerhof, Nucl. Phys. **A206**, 1 (1973).
[40] V. S. Vasilevskiĭ and Yu. I. Rybkin, Yad. Fiz. **46**, 419 (1987) [Sov. J. Nucl. Phys. **46**, 220 (1987)]; P. Ph. Vanderpeutte, Thesis, Faculté des Sciences, Univ. de l'Etat a Mons, Belgium (1984).
[41] G. M. Hale and D. C. Dodder, in *Proc. of the Tenth Intern. Conf. on Few-Body Problems in Physics*, edited by B. Zeitnitz (North-Holland, Amsterdam, 1984), Vol. 2, p. 434.
[42] F. Ajzenberg-Selove and C. L. Bush, Nucl. Phys. **A336**, 1 (1980).
[43] N. S. Zelenskaya and I. B. Teplov, *Exchange Processes in Nuclear Reactions* [in Russian] (Moscow State University Press, Moscow, 1985).
[44] V. Iskra, A. I. Mazur, V. G. Neudachin, and Yu. F. Smirnov, Yad. Fiz. **49**, 672 (1989) [Sov. J. Nucl. Phys. **49**, 416 (1989)].
[45] S. Mellema, T. R. Wang, and W. Haeberly, Phys. Lett. **166B**, 282 (1986).
[46] W. T. H. Van Oers and K. W. Brockman, Jr., Nucl. Phys. **A92**, 561 (1967); W. Trachlin, L. Brown, T. B. Clegg, and R. G. Seyler, Phys. Lett. **25B**, 585 (1967); J. Arvieux, Nucl. Phys. **A102**, 513 (1967); C. J. Clews and N. Berovic, Phys. Lett. **33B**, 347 (1970); R. Grotzschel, B. Kuhn, H. Kumpf *et al.*, Nucl. Phys. **A174**, 301 (1971); P. A. Schmeltzbach, W. Gruebler, R. G. White *et al.*, Nucl. Phys. **A197**, 273 (1972).
[47] J. Arvieux, Nucl. Phys. **A221**, 253 (1974).
[48] E. W. Schmid and H. Ziegelmann, *The Quantum Mechanical Three-Body Problem* (Pergamon Press, Oxford, 1974) [Russian transl., Nauka, Moscow, 1979].
[49] V. G. Neudachin, V. N. Pomerantsev, and A. A. Sakharuk, in *Proc. of the Intern. Seminar on Microscopic Methods in the Theory of Few-Particle Systems* [in Russian], Kalinin, August, 1988, edited by V. B. Belyaev and A. M. Gorbatov (Kalinin State University Press, Kalinin, 1988), p. 139.
[50] S. A. Sofianos, Phys. Rev. C **35**, 894 (1987).
[51] V. I. Kukulin and V. N. Pomerantsev, Yad. Fiz. **27**, 1668 (1978) [Sov. J. Nucl. Phys. **27**, 875 (1978)].
[52] T. A. Cahill, J. Greenwood, H. Willmes, and D. J. Shadoan, Phys. Rev. C **4**, 1499 (1971).
[53] J. C. Van der Weerd, T. R. Canada, C. L. Fink, and B. L. Cohen, Phys. Rev. C **35**, 66 (1971).
[54] V. G. Neudachin, V. N. Pomerantsev, and A. A. Sakharuk, Yad. Fiz. **52**, 738 (1990) [Sov. J. Nucl. Phys. **52**, 473 (1990)]; in *Proc. of the Seventh Seminar on Electromagnetic Interactions of Nuclei at Low and Intermediate Energies* [in Russian], Moscow, December, 1988 (Moscow, 1990), p. 154.
[55] B. Jenny, W. Gruebler, P. A. Schmelzbach *et al.*, Nucl. Phys. **A337**, 77 (1980); Yu. G. Balashko, Tr. Fiz. Inst. Akad. Nauk SSSR **32**, 4 (1964) [Proc. Lebedev Inst.].
[56] J. E. Brolley, Jr., T. M. Putnam, L. Rosen, and L. Stewart, Phys. Rev. **117**, 1307 (1960); M. Ivanovich, P. G. Young, and G. G. Ohlsen, Nucl. Phys. **A110**, 441 (1968); T. R. King and R. Smythe, Nucl. Phys. **A183**, 657 (1972).
[57] F. S. Chwieroth, R. E. Brown, Y. C. Tang, and D. R. Thompson, Phys. Rev. C **8**, 938 (1973).
[58] P. Heiss and H. H. Hackenbroich, Z. Phys. **231**, 230 (1970); Nucl. Phys. **A162**, 530 (1971).
[59] T. A. Tombrello, Phys. Rev. **138**, B40 (1965).
[60] D. H. McSherry and and S. D. Baker, Phys. Rev. C **1**, 888 (1970).
[61] R. Darves-Blanc, Nguyen Van Sen, J. Arvieux *et al.*, Nucl. Phys. **A191**, 353 (1972).
[62] J. R. Morales, T. A. Cahill, D. J. Shadoan, and H. Willmes, Phys. Rev. C **11**, 1905 (1975).
[63] B. T. Murdoch, D. K. Hasell, A. M. Sourkes *et al.*, Phys. Rev. C **29**, 2001 (1984); D. Muller, R. Beckmann, and U. Holm, Nucl. Phys. **A311**, 1 (1978).
[64] I. Reichstein, D. R. Thompson, and Y. C. Tang, Phys. Rev. C **3**, 2139 (1971); P. N. Shen, Y. C. Tang, H. Kanada, and T. Kaneko, Phys. Rev. C **33**, 1214 (1986).
[65] L. Beltramin, R. del Frate, and G. Pisent, Nucl. Phys. **A442**, 266 (1985).
[66] R. Kankowsky, L. C. Fritz, K. Kilian *et al.*, Nucl. Phys. **A263**, 29 (1976).
[67] R. A. Hardekopf, P. W. Lisowski, T. C. Rhea, and R. L. Walter, Nucl. Phys. **A191**, 481 (1972).
[68] J. L. Detch, Jr., R. L. Hutson, N. Jarmie, and J. H. Jett, Phys. Rev. C **4**, 52 (1971).
[69] Y. C. Tang, M. Le Mer, and R. D. Tompson, Phys. Rep. **37**, 167 (1978).
[70] A. N. Gorbunov, Tr. Fiz. Inst. Akad. Nauk SSSR **71**, 3 (1974) [Proc. Lebedev Inst.].
[71] C. A. Barnes, K. H. Chang, T. R. Donoghue *et al.*, Phys. Lett. **197B**, 315 (1987).
[72] W. K. Pitts, H. O. Meyer, L. C. Bland *et al.*, Phys. Rev. C **37**, 1 (1988).
[73] J. L. Langenbrunner, G. Feldman, H. R. Weller *et al.*, Phys. Rev. C **38**, 565 (1988).
[74] J. Piekarewicz and S. E. Koonin, Phys. Rev. C **36**, 875 (1987).
[75] G. Blude, H. J. Assenbaum, and K. Langanke, Phys. Rev. C **36**, 21 (1987).
[76] H. J. Assenbaum and K. Langanke, Phys. Rev. C **36**, 17 (1987).
[77] B. A. Craver, Y. E. Kim, and A. Tubis, Nucl. Phys. **A276**, 237 (1975).
[78] V. V. Kotlyar and A. V. Shebeko, Yad. Fiz. **45**, 984 (1987) [Sov. J. Nucl. Phys. **45**, 610 (1987)].
[79] B. Wachter, T. Mertelmeier, and H. M. Hofmann, Phys. Lett. **200B**, 246 (1988).
[80] V. I. Kukulin, G. G. Ryzhikh, Yu. M. Chuvil'skiĭ, and R. A. Éramzhyan, Izv. Akad. Nauk SSSR, Ser. Fiz. **53**, 121 (1989) [Bull. Acad. Sci. USSR, Phys. Ser.].
[81] M. M. Giannini and G. Ricco, Riv. Nuovo Cimento **8**, 1 (1985).
[82] T. De Forest and J. D. Walecka, Adv. Phys. **15**, 1 (1966).
[83] J. M. Eisenberg and W. Greiner, *Nuclear Theory, Vol. II: Excitation Mechanisms of the Nucleus* (North-Holland, Amsterdam, 1972) [Russian transl., Atomizdat, Moscow, 1973].
[84] I. Joenpera, *Matrix Elements for Spin Current Transitions in the Elastic Electroexcitations of Nuclei by Using Different Vector Potential Decompositions*, Ann. Acad. Sci. Fennicae, Ser. AIV Physica (1972).
[85] *A Theoretical Practicum on Nuclear and Atomic Physics* [in Russian], edited by V. V. Balashov (Energoatomizdat, Moscow, 1984).
[86] A. J. F. Siegert, Phys. Rev. **52**, 787 (1937).
[87] L. D. Landau and E. M. Lifshitz, *Quantum Mechanics* (Pergamon Press, Oxford, 1977) [Russian original, 4th ed., Nauka, Moscow, 1989].
[88] V. T. Voronchev, V. M. Krasnopol'sky, and V. I. Kukulin, J. Phys. G **8**, 649, 667 (1982).
[89] N. A. Burkova, M. A. Zhusupov, and R. A. Éramzhyan, Preprint P-0531, Institute of Nuclear Physics, USSR Academy of Sciences, Moscow (1987)[in Russian].
[90] N. A. Burkova, M. A. Zhusupov, and R. A. Éramzhyan, Preprint P-0551, Institute of Nuclear Physics, USSR Academy of Sciences, Moscow (1987)[in Russian].
[91] M. A. Zhusupov and Yu. N. Uzikov, Fiz. Elem. Chastits At. Yadra **18**, 323 (1987) [Sov. J. Part. Nucl. **18**, 136 (1987)].
[92] L. I. Schiff, Phys. Rev. **52**, 149 (1937).
[93] M. Verde, Helv. Phys. Acta **23**, 453 (1950).
[94] D. M. Skopik, H. R. Weller, N. R. Roberson, and S. A. Wender, Phys. Rev. C **19**, 601 (1979).
[95] B. L. Berman, L. J. Koester, and J. H. Smith, Phys. Rev. **133**, B117 (1964).
[96] J. R. Stewart, R. C. Morrison, and J. C. O'Connell, Phys. Rev. **138**, B372 (1965).
[97] S. K. Kundu, Y. M. Shin, and G. D. Wait, Nucl. Phys. **A171**, 384 (1971).
[98] H. Bock and H. Walenta, Z. Phys. **238**, 56 (1970).
[99] B. D. Belt, C. R. Bingham, M. L. Halbert, and A. Van der Woude,

Phys. Rev. Lett. **24**, 1120 (1970).
[100] U. Eichman, Z. Phys. **175**, 115 (1963).
[101] V. N. Fetisov, Nucl. Phys. **A98**, 437 (1967).
[102] R. Frascaria, V. Comparat, N. Marty *et al.*, Nucl. Phys. **A178**, 307 (1971).
[103] R. F. Wagner and C. Werntz, Phys. Rev. C **4**, 1 (1971).
[104] T. R. King, W. E. Meyerhof, and R. G. Hirko, Nucl. Phys. **A178**, 337 (1972).
[105] H. Paetzgen Schieck, Few-Body Syst. **5**, 171 (1988).
[106] H. R. Weller and D. R. Lehman, Ann. Rev. Nucl. Part. Sci. **38**, 563 (1988).
[107] G. E. Brown and A. D. Jackson, *The Nucleon–Nucleon Interaction* (North-Holland, Amsterdam, 1976) [Russian transl., Atomizdat, Moscow, 1979].
[108] M. D. Skopik and W. R. Dodge, Phys. Rev. C **6**, 43 (1972).
[109] B. Wachter, T. Mertelmeier, and H. M. Hofmann, Phys. Rev. C **38**, 1139 (1988).

Translated by Patricia A. Millard